

Commemoration of the centenary of the birth of S M Rytov (Scientific session of the Physical Sciences Division of the Russian Academy of Sciences, 26 November 2008)

Yu V Gulyaev; Yu N Barabanenkov; A E Kaplan, S N Volkov;
V I Klyatskin; L S Dolin

DOI: 10.3367/UFNe.0179.200905f.0531

A scientific session of the Physical Sciences Division of the Russian Academy of Sciences (RAS) was held in the Conference Hall of the P N Lebedev Physical Institute, RAS on November 26, 2008. The session was dedicated to the 100th anniversary of the birth of Sergei Mikhailovich Rytov.

The following reports were presented at the session:

(1) **Gulyaev Yu V** (V A Kotel'nikov Institute of Radioengineering and Electronics, RAS, Moscow) “Sergei Mikhailovich Rytov (Opening address)”;

(2) **Barabanenkov Yu N** (V A Kotel'nikov Institute of Radioengineering and Electronics, RAS, Moscow) “Asymptotic limit of the radiative transfer theory in problems of multiple wave scattering in randomly inhomogeneous media”;

(3) **Kaplan A E, Volkov S N** (Johns Hopkins University, Baltimore, USA) “Local fields in nanolattices of strongly interacting atoms: nanostrata, giant resonances, ‘magic numbers,’ and optical bistability”;

(4) **Klyatskin V I** (A M Obukhov Institute of Atmospheric Physics, RAS, Moscow) “Modern methods for the statistical description of dynamical stochastic systems”;

(5) **Dolin L S** (Institute of Applied Physics, RAS, Nizhny Novgorod) “Development of the radiative transfer theory as applied to instrumental imaging in turbid media”.

An abridge version of the reports is given below.

PACS numbers: **01.60.** + q, **01.65.** + g, 42.25.Bs

DOI: 10.3367/UFNe.0179.200905g.0531

Sergei Mikhailovich Rytov (Opening address)

Yu V Gulyaev

On July 3, 2008 we celebrated the 100th anniversary of the birth of Professor Sergei Mikhailovich Rytov — one of the outstanding Russian physicists in radiophysics and a Corresponding Member of the USSR Academy of Sciences.

Uspekhi Fizicheskikh Nauk **179** (5) 531 – 560 (2009)

DOI: 10.3367/UFNr.0179.200905f.0531

Translated by V I Kisin, S D Danilov, S N Volkov;
edited by A Radzig, A M Semikhatov



Sergei Mikhailovich Rytov
(03.07.1908 – 22.10.1996)

Sergei Mikhailovich obtained results of the paramount importance, which were recognized the world over in each field of physics where he worked — the theory of oscillations and acoustics, wave propagation, electrodynamics and optics, and, finally, statistical radiophysics. Some of these results became cornerstones of new fields in theoretical radiophysics. S M Rytov's work on parametric systems, the extension of the perturbation method, and its application to oscillator frequency stabilization belongs to the most prominent achievements of the Soviet school of the theory of nonlinear oscillations. Among other things he developed the

method of smooth oscillations (known in the literature as Rytov's method and widely used to study wave propagation in randomly inhomogeneous media) which constitutes one of the most essential results in the series of research programs covering the diffraction of light by ultrasound waves. In statistical radiophysics, S M Rytov's work which he summarized in a monograph, paved the way for a new domain in the theory of thermal fluctuation noise and thermal fluctuation fields that allows a unified consideration of thermal electromagnetic fields in the entire range of frequencies—from quasistationary to optical.

It would be forgivable to end the story with this brief list: brevity is acceptable when speaking about a great person. I will nevertheless remind the reader of the main stages in the biography of Sergei Mikhailovich, mostly for the sake of the younger generations, who never had a chance of having worked alongside him.

Sergei Mikhailovich Rytov was born on July 3, 1908 in Khar'kov. In 1930, he graduated from the Physics and Mathematics Department of Moscow State University (MGU), and in 1933 entered a postgraduate course at MGU under the guidance of Academician Leonid Isaakovich Mandel'shtam. It must be mentioned that later he brilliantly continued in his profession of a physicist and a teacher the best traditions of the scientific school of L I Mandel'shtam, whom he always considered his mentor. Sergei Mikhailovich taught young scientists to follow these wonderful traditions, one of which was infinite devotion to science and another, to always demand the utmost of yourself.

In 1934, Sergei Mikhailovich began working as a researcher of the 1st rank at the optics laboratory of the Lebedev Physical Institute (FIAN in *Russ. abbr.*) and later, from 1950 to 1958, he headed the theoretical sector of this laboratory. In 1958, at the request of Academician Aleksandr L'vovich Mints, Sergei Mikhailovich was transferred to the theoretical division of the Institute of Radio Engineering of the USSR Academy of Sciences (RTI in *Russ. abbr.*) where he worked until his last days.

Sergei Mikhailovich devoted all his life to research. His talent and passion for work led him to spectacular results and he became a recognized authority in many areas of physics, first and foremost radiophysics.

His study of the diffraction of light on ultrasound became one of the foundations of acousto-optics, which later went through vigorous expansion and had various practical applications. The method of smooth oscillations he had developed (known as Rytov's method) proved to be a very powerful tool for studying wave propagation in randomly inhomogeneous media. Later Sergei Mikhailovich, his students, and his followers successfully used this tool. The results they obtained are partly summarized in widely known review papers published in *UFN (Phys. Usp.)* (1970–1975) and in the latest issues of his *Introduction to Statistical Radiophysics*; they have also influenced monographs and reviews written by other authors. Some of the fundamental results obtained by Sergei Mikhailovich were used at RTI to begin important research on the effects of the troposphere and ionosphere of the Earth on the accuracy of long-range radar systems being developed and on evaluating their potential in the conditions of the real atmosphere.

Sergei Mikhailovich's DSc thesis entitled “Modulated oscillations and waves” enormously affected progress in the theory of oscillations and brilliantly demonstrated the fruitfulness of the oscillation-based approach to various

problems in physics. The thesis, published in the *Proceedings of the USSR FIAN* in 1940, became a desktop must for many researchers in oscillation theory. Sergei Mikhailovich continued working on the theory of oscillations and waves; he received important results on the theory of Thomson type self-induced oscillations, the theory of betatron and synchrotron oscillations, and the theory of parametric generators and amplifiers (1948–1963). He was the first to analyze the problem of resonance in parametric systems and he investigated the phenomenon of ‘pulling’ in the hard mode of the self-excitation of oscillations. His work on parametric systems, the extension of the perturbation method, and the application of this method to the problem of stabilization of generator frequency belong to the most important achievements of the Soviet school of the theory of nonlinear oscillations. His studies on the theory of oscillations were successfully extended by his numerous students and followers.

The theory of equilibrium thermal fluctuations of an electromagnetic field, developed by Sergei Mikhailovich and completed in collaboration with M L Levin, in which the classical reciprocity theorem ‘unexpectedly’ proved to be very efficient, led to a unified description of these fluctuations in the entire frequency range—from the quasistationary to the optical—and is widely used in a wide variety of fields of physics. The results of the theory were later generalized to the case of fields of any nature (1973).

Sergei Mikhailovich created the most general form of the phenomenological theory of the molecular scattering of light, which includes an analysis of Mandel'shtam–Brillouin spectra and depolarized radiation, as well as scattering spectra due to entropy fluctuations (1955–1970). This theory was confirmed by numerous experiments and earned general recognition.

It is also necessary to point out Sergei Mikhailovich's papers in which he for the first time gave a rigorous solution to the problem of reflection of electromagnetic waves from a layer with a negative dielectric constant, outlined the correct electrodynamic approach to the problem of wave propagation in tubes and generalized transmission lines with losses, considered a new type of phase diffraction structures, and achieved complete clarity on the question of the relation between the Poynting vector, the group velocity vector, and energy density when electromagnetic waves propagate through anisotropic media.

An inseparable part of Sergei Mikhailovich's creative activities was teaching; he loved doing it, teaching practically all his life and feeling the utmost responsibility to do so. The fact that he put this type of activity first on the list in his *Biographical data* is evidence of its significance in his life; he wrote that he started teaching already in 1928, while a 3rd-year student at MGU. Later he lectured in physics and mathematics at MGU and Gorky State University.

From 1947 on, practically to the end of his life, Sergei Mikhailovich Rytov held a part-time position at the Moscow Institute of Physics and Technology¹ as professor at the Chair of General Physics (until 1949) and then professor at the Chair of Radiophysics. He headed this Chair from 1953 till 1978 (i.e., for 25 years).

Everyone who heard Sergei Mikhailovich lecture at least once felt in awe of his art of lecturing, the honed form of

¹ MFTI in *Russ. abbr.*, until 1951—The Physics and Engineering Department of MGU.

delivery, and his clarity, profoundness, and at the same time simplicity of presentation. Students loved their professor, and attending his lectures was a pleasure; after sitting for his exam they invariably left with a feeling of satisfaction regardless of the mark awarded: he was always correctness itself and impeccably fair.

I was one of those lucky students, attending his course 'Theory of Oscillations', and even got my 'excellent' mark from him personally. Like other students, I jotted down the synopsis of all the lectures of his course; in my later work in the field of oscillation theory and microwave acoustics I would hardly need any other source: Sergei Mikhailovich's course was that complete and that clear.

The pinnacle of Sergei Mikhailovich's pedagogical creativity was his course of lectures on statistical radiophysics, which he wrote and then brilliantly delivered for many years at MFTI. Here for the first time he came up with the most laconic and rich definition of radiophysics: "This is physics for radio plus radio for physics," which legitimized radiophysics in the company of related subjects. On the basis of these lectures, he wrote the first textbook in the world on statistical radiophysics for higher education — *An Introduction to Statistical Radiophysics* (1966), which gained high reputation both in this country and abroad.

Sergei Mikhailovich took active part in writing the physics textbooks whose editor-in-chief was N D Papaleksi (1939–1948), and the *Elementary Physics Textbook* whose editor-in-chief was G S Landsberg. Sergei Mikhailovich was editor-in-chief of 15 books, three of them being translations into Russian.

For a long time, from 1953, Sergei Mikhailovich had served as permanent head of the All-Moscow Radiophysics Seminar, which played an enormously important role in the progress of radiophysics in this country. Scientists from many scientific centers in the country took part regularly in the work of the seminar, so that in reality this was an All-Union seminar. The popularity and the high rating of the seminar stemmed most of all from the decisive scientific reputation enjoyed by Sergei Mikhailovich, from his ability to provide an expert evaluation of a contribution and to lucidly formulate its stronger and weaker points. The seminar was purely scientific, devoid of any official functions or formalities. The only 'official document' was the agenda with presentation titles and speakers' names, which was sent out to participants in advance by the secretary of the seminar. The meetings followed democratic rules ably controlled by Sergei Mikhailovich.

The seminar was the center of attraction not only for radiophysicists but also for specialists in the most varied fields of physics interested in methodology and the results of radiophysics research. It would be difficult to name any important new field in radiophysics that would not have been represented at the seminar. It was here that many research areas were given a nod of approval. The seminar was a real scientific school for its young participants. This was stimulated by a very special atmosphere of genuine devotion to science, an attitude of goodwill, and the inoffensive humour that Sergei Mikhailovich demonstrated during the sessions. It is not surprising therefore that not only Rytov's immediate students and staff members but also many others who benefited from contacts with Sergei Mikhailovich regarded themselves as members of his school.

Sergei Mikhailovich worked at RTI—the institute created for the purpose of solving defense-related problems of

national importance—for more than 35 years, beginning from 1958. His work in the framework of RTI defense projects targeted principally important physics aspects that involved developing and designing ground-based high-aperture radioinformation complexes. People tried not to bother him with trifles. He initiated, and took active part in, a number of new areas of research important for RTI primary tasks.

We already mentioned that one of the areas in which S M Rytov worked was to find out how nonuniformity of the atmosphere affected the characteristics of long-range radars. We can also mention such fields as the development and design of low-noise parametric amplifiers, extension of acousto-optical methods for processing radar signals, the study of the ionosphere by means of rockets and artificial Earth satellites in the interest of long-haul radiolocation, etc.

In situations of dispute, S M Rytov occasionally acted as a highly respected arbiter. His opinion was invariably profoundly reasoned and scientifically sound, which made it possible to avoid mistaken or adventurist technical solutions, however attractive they may have seemed at first glance. He was often approached to obtain advice and consultation by directors' offices, by heads of departments, or by lower-rank staff members. No one was refused. His reports on important areas of research in science and technology at RTI seminars for large audiences of RTI staff are well remembered. The Laboratory of Theoretical Radiophysics that he headed was a center of attraction for talented creative young generations, first and foremost students and postgraduates of the base Chair of Radiophysics at MFTI; many of them later came to obtain CandSc and DSc degrees or became science managers and leading specialists in this country.

Sergei Mikhailovich was generous with his knowledge and his experience in the social activities of research institutions: he was a member of the Learned Councils of MFTI and RTI and of the editorial board of the journal *Radiotekhnika i Elektronika* [Radioengineering and Electronics]; sat on the Methodological Council on Physical and Mathematical Sciences of the All-Union Society 'Znanie' (Knowledge), the Interdepartmental Research and Development Council on Sun–Earth issues², and the Bureau of the Learned Council of the USSR Academy of Sciences for the complex problem the Propagation of Radiowaves; chaired a section of the Learned Council of the USSR Academy of Sciences on the issue of Statistical Radiophysics, etc.

For his outstanding contributions to science and industry S M Rytov was awarded the A S Popov Gold medal, the L I Mandel'shtam Prize, and the State Prize, and received many distinguished orders and medals.

Commemorating now the 100th anniversary of the birth of Sergei Mikhailovich Rytov, we remember with gratitude the enormous contribution he made to the inception and progress of radiophysics and related fields of science, to the formation of the school of radiophysics in this country, and to nurturing and training of new generations of scientists. He was uniquely devoted to science and had brilliant pedagogical skills and enviable human qualities. S M Rytov's name occupies a well-deserved place in the gallery of classic personalities of science in this country and abroad.

More detailed information on the life and scientific career of Sergei Mikhailovich Rytov can be found in the editorial of

² Renamed in 1978 the Learned Council of the USSR Academy of Sciences for the issue of Solar–Terrestrial Relations.

the special issue of the journal *Electromagnetic Waves and Electronic Systems* devoted to the 100th anniversary of the birth of this brilliant scientist.

PACS numbers: 42.25.Bs, 42.25.Dd, 72.15.Rn
DOI: 10.3367/UFNe.0179.200905h.0534

Asymptotic limit of the radiative transfer theory in problems of multiple wave scattering in randomly inhomogeneous media

Yu N Barabanenkov

1. Introduction

Wave propagation in disordered systems is considered one of the most difficult subjects of theoretical physics. The traditional approach involves the phenomenological radiative transfer theory [1, 2], which originated more than a century ago in the studies by Khvol'son (1890), Schuster (1905), and Schwarzschild (1906) devoted to light scattering in milk glasses and solar and foggy earth atmospheres; it is based on the notions of linear kinetic theory involving an elementary scattering act and radiation free path. In the 1950s, the development of the theory of partial coherence for wave fields prompted active studies of the applicability limits for the radiative transfer theory from the standpoint of the statistical theory of multiple wave scattering in randomly inhomogeneous media. Their results were regularly reported and critically discussed at the All-Moscow Radiophysics Seminar headed by S M Rytov from 1965 to 1985. Although this research was purely theoretical, it resulted in the prediction of weak light localization in randomly inhomogeneous media in 1973. Because this phenomenon lay at the applicability boundary of the radiative transfer theory, it could not be ignored.

As early as 1967, a derivation was proposed [3] (see also [4]) of the phenomenological radiative transfer equation in a discrete randomly inhomogeneous medium, with due regard for the correlation of scatterers in all orders and mutual irradiation of scatterers within the same effective inhomogeneity, i.e., a cluster of scatterers. A single scatterer was characterized by its shape, dielectric permeability, and conductivity; the method of Dyson and Bethe–Salpeter equations, the Feynman diagram technique, and the concept of the quantum mechanical scattering operator were used [5]. The transfer equation [3], with pair correlation of weak scatterers satisfying the applicability conditions of the Born approximation taken account, was used to investigate an increase in the free path length of microwaves in snow layers and conduction electrons in liquid metals [6], as well as the opposite effect of a decrease in the free path of light [7] and neutrons in a liquid [6] in the vicinity of a phase transition critical point. The contribution from higher correlations of weak scatterers to the light free path at critical opalescence was considered in Ref. [8], while Ref. [9] dealt with the influence of higher correlations due to large, optically dense scatterers on the transmittance of a layer composed of such particles.

Simultaneously with the derivation of the transfer equation [3], the applicability condition for the phenomenological

transfer theory was formulated as the single-group approximation, i.e., the possibility to discard all repeated scattering of radiation on the same inhomogeneity. Additionally, it is required that inhomogeneities be in the far field of Fraunhofer diffraction with respect to each other. The first part of this condition, later called the approximation of independent scattering on effective inhomogeneities [10], disregards all loops in multiple wave scattering with a diameter of the order of or larger than the free path length of radiation.

The decisive role of the single-group approximation for the transfer theory was convincingly demonstrated with the model of multiple scattering of a nonstationary wave field in a randomly inhomogeneous and randomly variable medium, for which the concept of a finite ‘lifetime’ of an inhomogeneity can be introduced. From this model, thoroughly studied in Refs [6, 11], the transfer theory follows as an asymptotically exact Van Hove limit [12] under the condition that the ratio of the inhomogeneity lifetime to the radiation free path time tends to zero, but the ratio of the observation time to the free path time remains fixed. The second condition of the Van Hove limit prevents repeated scattering due to a selected inhomogeneity from occurring on a large time or space scale of radiation propagation. In repeated scattering, the effects of multi-group or dependent scattering, i.e., the loops, would have to be taken into account, and the phenomenological radiative transfer theory would need modifications.

The most thoroughly studied effect of multi-group or dependent scattering by effective inhomogeneities is manifested through the coherent enhancement of backscattering. It was first predicted as a wave correction to the solution of the transfer equation for scattering directed exactly ‘backward’ [13]. Reference [14] shows, based on the technique of cyclic (maximally crossed) Feynman diagrams, that the wave correction attains a relative value close to unity in a narrow backscattering cone whose angular width is of the order of the ratio of the wave length to the free path length of radiation.

The predicted cone of enhanced backscattering was experimentally observed by several groups [15–17]. It strongly stimulated research on the weak localization phenomenon in optics [18]. Coherent enhanced backscattering stems from coherent loops in which the field and its complex conjugate go around a given set of inhomogeneities in opposite ways. There also exist incoherent loops, in which case a set of inhomogeneities is passed by the field and its complex conjugate in the same order. The incoherent loops lead to the backscattering effect for nonstationary radiation in a modified transfer theory with time delay [19], where the delay time is of the order of the radiation free path time. Another variant of the transfer theory with time delay emerges on considering the effect of trapping [20] under multiple scattering of wave radiation, for example, a short femtosecond laser pulse [21], in a randomly inhomogeneous medium composed of resonant scatterers.

Taking account of loops in multiple wave scattering implies lifting the part of the applicability condition of the phenomenological transfer equation [3] that requires omitting repeated scattering of radiation by the same inhomogeneity. No principal obstacles are seen in using this equation to explore multiple light scattering by new artificial systems such as statistical ensembles of nanoclusters [22], in which each cluster represents a combination of a possibly large but finite number of atoms (or molecules) and requires describing light scattering with methods of quantum mechanics or

electrodynamics. Admittedly, it may call for considering effects from near fields in the form of evanescent waves in some vicinity of effective inhomogeneities (nanoclusters), i.e., abandoning the condition that the inhomogeneities are located in the far wave zone of Fraunhofer diffraction with respect to each other.

Recently, considerable progress has been achieved in the theoretical understanding of the role played by near fields in multiple scattering of electromagnetic waves by inhomogeneous dielectric media. The progress was facilitated by using the Sommerfeld–Weyl representation for angular spectral amplitudes of local electromagnetic waves propagating along and against the axis of the parameter of embedding into a layer of a three-dimensional medium, and by exploring the phenomenon of energy emission from an evanescent wave scattered by a dielectric structure [23], with checks for the extended unitarity of the 2×2 block S -matrix [24] and the interpretation of the mentioned energy emission through the interference of two evanescent waves decaying toward each other [25]. As a result, an approach was formulated [26] to establishing a modified theory of electromagnetic radiation transfer in a randomly inhomogeneous medium with the effects of near fields and interference of oppositely directed wave beams taken into account.

Finally, perspectives of exploring the electrodynamic properties of artificial materials exemplified by statistical ensembles of particles with a given shape, dielectric permeability and conductivity (see, e.g., Ref. [27]), and, possibly, high spatial packing parameter, put forward the task of radically modifying the phenomenological radiative transfer theory while preserving some of its properties. Such a modification hinges on the Ambartsumyan method of layer summation [28], according to which the scattering medium is split in virtual layers (slices) separated by small gaps, with a subsequent derivation of transfer relations in terms of the intensity between radiation fluxes in gaps and the fluxes reflected from and transmitted through the entire medium.

The idea about the virtual layering of the medium into slices and gaps is evidently applicable to any medium, in particular, that consisting of the particles mentioned previously, for further derivation of transfer relations between the radiation fluxes, and not only for wave intensities but also for wave amplitudes, as in Refs [29, 30]. The transfer relations obtained there imply a system of four differential Riccati equations for the blocks of the S -matrix, written for a layer of a medium in the form of Reid [31] and Redheffer [32], with differentiation over the parameter of embedding into the layer. Using the Reid method, a relation is established between the solution of the system of nonlinear matrix Riccati equations and that of the linear differential equation for the transfer matrix. Paper [30] elaborates on the extended relations of unitarity and invariance under time reversal for the solution of the system of Riccati equations and of the transfer matrix equation. The extended relations augment, by near-field effects, the more habitual quantum mechanical relations used in the widely known theory for the transmission coefficient and electron localization length in N connected disordered chains developed by Dorokhov [33] and the authors of Ref. [34] based on the Fokker–Planck equation for the probability distribution function for transfer matrix elements.

Noteworthy in the just mentioned system of matrix Riccati equations is the fact that the governing role belongs to the equation for the coefficient of wave reflection from a

layer of a three-dimensional randomly inhomogeneous dielectric medium written for angular spectral amplitudes, which is independent of the other equations. It was studied in [35] and served as a starting point in Ref. [36], where the functional Fokker–Planck equation for the functional of the probability distribution of the reflection coefficient was written.

The treatment of the Fokker–Planck equation in variational derivatives is exceptionally difficult. However, one can change to ordinary derivatives by discretizing the space of the wave vector transverse to the axis of the embedding parameter, in analogy with the method of the transfer matrix with a finite number of propagation channels in the quantum mechanical theory dealing with interference effects in metal conductors [37].

In exploring multiple wave scattering by statistical ensembles of particles characterized by a large packing parameter, it seems reasonable to assume that the distribution of particles is periodic in the zeroth approximation, as in the structure of the photon crystal [38]. In this case, for example, the matrix Riccati equation for the reflection coefficient turns out to be naturally discretized over diffraction orders of the radiation reflected from and transmitted through the structure layer. This equation was successfully used in Ref. [39] for numerical computation via the Runge–Kutta method of formation of gaps in the spectrum of radiation transmission through an ordered system of dielectric cylinders with arbitrary cross sections.

Some of the aforementioned questions of the asymptotic limit of the radiative transfer theory are considered in detail in what follows.

2. Single-group approximation and the Van Hove limit

In the scalar case, the phenomenological transfer equation written for the ray intensity $I(\mathbf{R}, \mathbf{s})$ at a point \mathbf{R} in the direction of a unit vector \mathbf{s} takes the form

$$\mathbf{s} \nabla I(\mathbf{R}, \mathbf{s}) = -\frac{1}{l} I(\mathbf{R}, \mathbf{s}) + \int_{4\pi} d\mathbf{s}' W(\mathbf{s}, \mathbf{s}') I(\mathbf{R}, \mathbf{s}'). \quad (1)$$

The coefficients of extinction $1/l$ and scattering $W(\mathbf{s}, \mathbf{s}')$ due to an elementary volume are expressed by via Fourier transformation through the mass operator M_1 and intensity operator K_1 of the Dyson and Bethe–Salpeter equations in the single-group approximation. They are symbolically represented by the series

$$\frac{M_1}{K_1} = \sum_{n=1}^{\infty} \frac{1}{n!} \int d\mathbf{l} \dots \int d\mathbf{n} g_n(1, \dots, n) (T_{1\dots n} \otimes T_{1\dots n}^*)^{\text{gr}}. \quad (2)$$

Here, natural numbers $1, \dots, n$ label spatial coordinates of points, $T_{1\dots n}$ is the operator of scattering by a system of n scatterers centered at these points, and $g_n(1, \dots, n)$ is the correlation function of the scatterers. The group subtraction operation gr removes small orders of scattering in the group of scatterers and acts in the simplest case as $T_{12}^{\text{gr}} = T_{12} - T_1 - T_2$. The symbol \otimes denotes the tensor product.

Originally, single-group approximation (2) was derived using the Feynman diagram technique. However, it was recognized later that it could be obtained on a purely analytic level, based on the exact Bethe–Salpeter relation [20, 40] of the

form

$$\begin{aligned} & (\mathbf{L} \otimes I - I \otimes \mathbf{L}) \langle G \otimes G^* \rangle \\ &= \left\langle [\mathbf{M} \otimes I - I \otimes \mathbf{M}^* - (G \otimes I - I \otimes G^*) \mathbf{K}] G \otimes G^* \right\rangle \\ &+ I \otimes \langle G^* \rangle - \langle G \rangle \otimes I, \end{aligned} \quad (3)$$

where \mathbf{L} is the differential operator of the wave equation in free space, G is the Green's function of the wave equation in a randomly inhomogeneous medium, and the angular brackets denote averaging over the statistical ensemble of scatterers. The operators \mathbf{M} and \mathbf{K} formally have the same analytic structure as the mass and intensity operators in single-group approximation (2), except for the replacement of the T operators of free space scattering with self-consistent random operators of scattering in a randomly inhomogeneous medium.

We assume that the random Green's function $G(\mathbf{r}, \mathbf{r}')$ satisfies the locality property and hence differs only slightly from its ensemble mean and the Green's function in free space if the distance between the observation and source points \mathbf{r} and \mathbf{r}' is of the order of the scatterer radii and their correlation radii. In that case, the random operators \mathbf{M} and \mathbf{K} practically coincide, respectively, with the mass and intensity operators in single-group approximation (2), while relation (3) transforms into the Bethe–Salpeter equation in the form of a kinetic equation [20].

The locality property of the random Green's function formulated above, in particular, implies omission of all loops in multiple wave scattering with a diameter of the order of or greater than the free path length of radiation. Can this property be justified in an asymptotically exact way? Such justification is known, for example, for the problem of the propagation of a quantum mechanical stream of particles in the field of a randomly varying potential $V(\mathbf{r}, t)$. Based on the stochastic Liouville–von Neumann equation for the density matrix $\rho(t)$ of a particle stream under the assumption that the probability distribution of random potential realizations is Gaussian, the kinetic equation for the ensemble mean density matrix $\bar{\rho}(\mathbf{R}, \mathbf{k}, t)$ in the Wigner variables was derived in Refs [6, 20] in the form

$$\begin{aligned} & \left(\frac{\partial}{\partial t} + \frac{\hbar \mathbf{k}}{m} \nabla_{\mathbf{R}} \right) \bar{\rho}(\mathbf{R}, \mathbf{k}, t) \\ &= \int d\mathbf{k}' W(\mathbf{k}, \mathbf{k}') [\bar{\rho}(\mathbf{R}, \mathbf{k}', t) - \bar{\rho}(\mathbf{R}, \mathbf{k}, t)]. \end{aligned} \quad (4)$$

Equation (4) is asymptotically exact in the Van Hove limit $\tau_0/t_M \rightarrow 0$, $t/t_M = \text{const}$, where t_M estimates the relaxation time t_r of the kinetic equation from below and the lifetime τ_0 of the effective inhomogeneity is expressed in terms of the cumulant of random potential fluctuations. Paper [11] considers the passage from kinetic equation (4) to the limit of stationary transfer equation (1) through the replacement of the observation time with the absorption time in the second condition of the Van Hove limit.

3. Coherent loops and weak localization

Coherent loops are linked to cyclic Feynman diagrams of the intensity operator [14]. Cyclic diagrams are omitted when transfer equation (1) is derived in the framework of single-group approximation (2). Nevertheless, they are, in some sense, equivalent to ‘ladder’ diagrams, which constitute the

main element of the transfer theory. This equivalence property follows upon inversion of the upper or lower rows of a cyclic diagram and using the reciprocity property of the Green's function and of the intensity operator in the single-group approximation. The equivalence property of cyclic diagrams enabled the author of Ref. [14] to conclude that there exists a cone of enhanced backscattering with the width $\delta\theta \approx \lambda/l$ measured by the ratio of the wavelength λ to the free path length l .

It is worth noting that Ref. [14] was published in relation to the discussion of the work by Gazaryan [41] which, based on the exact solution to the Anderson strong localization problem [42] in a one-dimensional randomly inhomogeneous medium, demonstrated, following Ref. [43], an exponentially fast decay of the layer transmittance for the mean intensity as a function of the layer thickness, instead of a power-law decay predicted by the transfer equation [1]. In other words, the transfer equation provides a reduced value for the reflective capability of the one-dimensional scattering layer. The goal of Ref. [14] was to demonstrate the reduction of a similar type in the framework of transfer theory for the reflective capability of a three-dimensional scattering layer, although a reduction in a weak sense.

4. Near fields and the tunnel component of radiative transfer

Near fields arise during multiple wave scattering in a randomly inhomogeneous medium as evanescent waves in the vicinity of effective inhomogeneities and participate in a specific way in radiation transfer together with propagating waves. Only the latter are taken into account by the phenomenological transfer theory. The principal role is here played by a formula derived in Ref. [25] for the radiation energy flux in an inhomogeneous dielectric medium. In the scalar version, this formula has the form

$$\begin{aligned} P_z(z) = & \int_{\mathbf{k}_\perp} H^{\text{pr}}(k_\perp) [\rho_{11}(\mathbf{k}_\perp, \mathbf{k}_\perp; z) - \rho_{22}(\mathbf{k}_\perp, \mathbf{k}_\perp; z)] \\ & + \int_{\mathbf{k}_\perp} iH^{\text{ev}}(k_\perp) [\rho_{12}(\mathbf{k}_\perp, \mathbf{k}_\perp; z) - \rho_{21}(\mathbf{k}_\perp, \mathbf{k}_\perp; z)], \end{aligned} \quad (5)$$

where $P_z(z)$ is the component of the Poynting vector along the z axis of the parameter of embedding into the medium layer $0 < z < L$, integrated in the plane perpendicular to this axis, $\rho_{mm'}(\mathbf{k}_\perp, \mathbf{k}'_\perp; z)$ is the density matrix [25] of (slowly varying) angular spectral amplitudes of local waves propagating in forward (index 1) and backward (index 2) directions relative to the z axis ($m, m' = 1, 2$), \mathbf{k}_\perp and \mathbf{k}'_\perp are the components of \mathbf{k} and \mathbf{k}' perpendicular to the z axis, $H^{\text{pr}}(k_\perp)$ and $H^{\text{ev}}(k_\perp)$ are the respective projectors on the propagating ($k_\perp < k_0$) and evanescent ($k_\perp > k_0$) waves, for which the longitudinal wave number $\gamma_k = [k_0^2 - k_\perp^2]^{1/2}$ takes a real or a purely imaginary value, and k_0 is the wave number of free space; the compact notation for integrals, $\int_{\mathbf{k}_\perp} = (2\pi)^{-2} \int d\mathbf{k}_\perp$, is used.

According to formula (5), the contribution of propagating waves to the total energy flux along the z axis is determined by intensities of angular spectral amplitudes of waves propagating in forward and backward directions, whereas the contribution of evanescent waves to this energy flux is expressed through the term corresponding to the interference of two evanescent waves decaying toward each other. Turning to a randomly inhomogeneous medium, we need to consider the coherence matrix for angular spectral amplitudes of local

waves for two values of the parameter of embedding into the medium, $\bar{\rho}_{mm'}(\mathbf{p}, \mathbf{p}'; z, z')$, where the bar denotes ensemble averaging and the short notation \mathbf{p} and \mathbf{p}' is used instead of \mathbf{k}_\perp and \mathbf{k}'_\perp . The Bethe–Salpeter equation for this coherence matrix with the mass and intensity operators is derived in single-group approximation (2).

In the simplest case of weak uncorrelated scatterers, we arrive at the model of a medium with Gaussian fluctuations of the potential, used in Ref. [26] to analyze effects of near fields in the transfer theory. After some simplification, the Bethe–Salpeter equation for the coherence matrix of angular spectral amplitudes is reduced to four equations, two of which allow computing ensemble-averaged intensities of angular spectral amplitudes for the forward and backward directions, and the other two, for complex-conjugate mutual coherences of evanescent waves decaying toward each other. One of the first two equations has the form

$$\begin{aligned} \hat{\rho}_{11}(\mathbf{p}, \mathbf{p}; z, z) = & \exp(-2\Im\gamma_{1p}z) |f(\mathbf{p})|^2 \\ & + \int_0^z dz_1 \exp[-2\Im\gamma_{1p}(z-z_1)] \int_{\mathbf{p}'} \frac{1}{4|\gamma_p||\gamma_{p'}|} \\ & \times [B(\mathbf{p}-\mathbf{p}', \gamma_p-\gamma_{p'}) \hat{\rho}_{11}(\mathbf{p}', \mathbf{p}'; z_1, z_1) \\ & + B(\mathbf{p}-\mathbf{p}', \gamma_p+\gamma_{p'}) \hat{\rho}_{22}(\mathbf{p}', \mathbf{p}'; z_1, z_1) \\ & + B(\mathbf{p}-\mathbf{p}', \gamma_p-\gamma_{p'}) \hat{\rho}_{12}(\mathbf{p}', \mathbf{p}'; z_1, z_1) \\ & + B(\mathbf{p}-\mathbf{p}', \gamma_p+\gamma_{p'}) \hat{\rho}_{21}(\mathbf{p}', \mathbf{p}'; z_1, z_1)]. \end{aligned} \quad (6)$$

Equation (6) is written in terms of the coherence matrix of rapidly varying angular spectral amplitudes $\hat{\rho}_{mm'}(\mathbf{p}, \mathbf{p}'; z, z') = \exp(i\zeta_m\gamma_{pz} - i\zeta_{m'}\gamma_{p'z}^*) \bar{\rho}_{mm'}(\mathbf{p}, \mathbf{p}'; z, z')$ with $\zeta_1 = 1$ and $\zeta_2 = -1$. The quantity $\Im\gamma_{1p}$ represents the imaginary part of the longitudinal wave number in a deterministic medium with the effective complex wave number k_1 ; it is assumed that a propagating wave with the angular spectral amplitude $f(\mathbf{p})$ is incident on the left layer boundary. The function $B(\mathbf{k}_\perp, k_z)$ is the three-dimensional Fourier transform of the cumulant of random potential fluctuations. Equation (6) describes multiple scattering of ensemble-averaged intensities of angular spectral amplitudes by effective inhomogeneities with a free path between them that is typical of the transfer theory. In addition, this equation, evidently, contains the contribution to mean intensity of waves propagating forward brought about by mutual coherences of evanescent waves as they are scattered on effective inhomogeneities.

The equation for computing the ensemble-averaged intensity of angular spectral amplitudes for waves propagating backward is similar to Eqn (6) and is not reproduced here.

We turn to the equation for mutual coherence of pairs of evanescent waves decaying toward each other, of the form

$$\begin{aligned} \hat{\rho}_{12}(\mathbf{p}, \mathbf{p}; z, z) = & \int_0^z dz_1 \int_z^L d\zeta_1 \exp[i\gamma_{1p}(z-z_1)] \\ & \times \exp[i\gamma_{1p}^*(z-\zeta_1)] \int_{\mathbf{p}'} \frac{1}{4|\gamma_p||\gamma_{p'}|} \\ & \times B(\mathbf{p}-\mathbf{p}', z_1-\zeta_1) \sum_{m,n} \exp[-i\zeta_m\gamma_{p'}(z-z_1)] \\ & \times \exp[i\zeta_n\gamma_{p'}^*(z-\zeta_1)] \hat{\rho}_{mn}(\mathbf{p}', \mathbf{p}'; z, z), \end{aligned} \quad (7)$$

where $B(\mathbf{k}_\perp, z)$ is the two-dimensional Fourier transform of the cumulant of random potential fluctuations in the plane perpendicular to the z axis.

Equation (7) differs principally from Eqn (6) by its structure. Indeed, the inequality $z_1 < z < \zeta_1$ holds in the double integral in the right-hand side of Eqn (7), with $\zeta_1 - z_1 \approx r_0$, where r_0 is the spatial scale of effective inhomogeneities. This implies that the observation point z and two scattering points z_1 and ζ_1 are confined to the same inhomogeneity, whereas two elementary evanescent waves appearing during scattering decay in the directions toward each other with interference at the observation point. This interference leads, as follows from a more detailed analysis of Eqn (7), to the following tunnel component of the radiation energy flux:

$$\begin{aligned} & -2 \int_{\mathbf{p}(k_0 < p < p_0)} \Im \hat{\rho}_{12}(\mathbf{p}, \mathbf{p}; z, z) \\ & = \frac{g}{1-g} \int_{\mathbf{p}(p < k_0)} [\hat{\rho}_{11}(\mathbf{p}, \mathbf{p}; z, z) - \hat{\rho}_{22}(\mathbf{p}, \mathbf{p}; z, z)]. \end{aligned} \quad (8)$$

Solution (8) of the imaginary part of Eqn (7) is obtained in the limit of small-scale fluctuations of the random potential, when two evanescent waves, one incident on the inhomogeneity and the other scattered by it, decay only slightly on the inhomogeneity scale, $|\gamma_p|r_0 \ll 1$ and $|\gamma_{p'}|r_0 \ll 1$, with $k_0 < p < p_0$ and $k_0 < p' < p_0$, where $p_0 \approx 1/r_0$ is some cut-off parameter. The parameter of the tunnel component of the energy flux is of the order of $g \approx r_0/l$, which represents the ratio of the inhomogeneity scale to the free path length, defined as $1/l = \langle V^2 \rangle r_0^3$. The observation point z is assumed to be located far enough from the layer boundaries with respect to the scale of the effective inhomogeneity.

Equality (8) demonstrates the existence of a homogeneous tunnel energy flux in a randomly inhomogeneous medium. It is proportional to the energy flux of propagating waves, as is common in the phenomenological transfer theory. In a weakly scattering medium, the proportionality coefficient is small compared to unity. However, in a medium with strong scattering, for example, the one consisting of resonant scatterers, the proportionality coefficient may increase in absolute value.

5. Conclusions

Elucidation of the applicability bounds for the phenomenological radiative transfer theory from the standpoint of the statistical theory of multiple wave scattering has led to the prediction and discovery of the phenomenon of weak light localization in a randomly inhomogeneous medium. The proposed modifications to the transfer theory have enabled the treatment of phenomena such as the trapping of radiation in a resonant medium and the tunnel transfer of radiation energy by near fields of effective scattering inhomogeneities. The ideas and methods of the transfer theory were fruitful in studies dealing with the formation of forbidden zones in spectra of radiation transmission through photon crystals and can be used to explore multiple light scattering by statistical ensembles of nanoclusters and conducting particles with a large packing parameter.

This work was supported in part by the Russian Foundation for Basic Research grant 06-02-17451.

References

1. Sobolev V V *Perenos Luchistoi Energii v Atmosferakh Zvezd i Planet* (A Treatise on Radiative Transfer) (Moscow: Gostekhizdat, 1956) [Translated into English (Princeton, NJ: Van Nostrand, 1963)]
2. Chandrasekhar S *Radiative Transfer* (New York: Dover Publ., 1960)
3. Barabanenkov Yu N, Finkel'berg V M *Zh. Eksp. Teor. Fiz.* **53** 978 (1967) [*Sov. Phys. JETP* **26** 587 (1968)]
4. Barabanenkov Yu N *Usp. Fiz. Nauk* **117** 49 (1975) [*Sov. Phys. Usp.* **18** 673 (1975)]
5. Goldberger M L, Watson K M *Collision Theory* (New York: Wiley, 1964)
6. Barabanenkov Yu N, Ozrin V D, Kalinin M I *Asimptoticheskie Metod v Teorii Stokhasticheskikh Lineinykh Dinamicheskikh Sistem (Asymptotic Method in the Theory of Stochastic Linear Dynamical Systems)* (Moscow: Energoatomizdat, 1985)
7. Barabanenkov Yu N, Stainova E G *Opt. Spektrosk.* **63** 362 (1987) [*Opt. Spectrosc.* **63** 211 (1987)]
8. Barabanenkov Yu N, Stainova E G *Opt. Spektrosk.* **59** 1342 (1985) [*Opt. Spectrosc.* **59** 803 (1985)]
9. Barabanenkov Yu N, Kalinin M I *Izv. Vyssh. Uchebn. Zaved. Radiofiz.* **29** 913 (1986) [*Radiophys. Quantum Electron.* **29** 701 (1986)]
10. Lagendijk A, van Tiggelen B A *Phys. Rep.* **270** 143 (1996)
11. Barabanenkov Yu N *Dokl. Akad. Nauk SSSR* **295** 79 (1987) [*Sov. Phys. Dokl.* **32** 556 (1987)]
12. van Hove L *Physica* **21** 517 (1954)
13. Watson K M *J. Math. Phys.* **10** 688 (1969)
14. Barabanenkov Yu N *Izv. Vyssh. Uchebn. Zaved. Radiofiz.* **16** 88 (1973) [*Radiophys. Quantum Electron.* **16** 65 (1973)]
15. Kuga Y, Ishimaru A *J. Opt. Soc. Am. A* **1** 831 (1984)
16. Van Albada M P, Lagendijk A *Phys. Rev. Lett.* **55** 2692 (1985)
17. Wolf P-E, Maret G *Phys. Rev. Lett.* **55** 2696 (1985)
18. van Rossum M C W, Nieuwenhuizen Th M *Rev. Mod. Phys.* **71** 313 (1999)
19. Barabanenkov Yu N, Ozrin V D *Izv. Vyssh. Uchebn. Zaved. Radiofiz.* **28** 450 (1985) [*Radiophys. Quantum Electron.* **28** 305 (1985)]
20. Barabanenkov Yu N, in *Wave Scattering in Complex Media: from Theory to Applications* (Eds B A van Tiggelen, S E Skipetrov) (Dordrecht: Kluwer Acad. Publ., 2003) p. 415
21. Vreeker R et al. *Phys. Lett. A* **132** 51 (1988)
22. Kresin V Z, Ovchinnikov Yu N *Usp. Fiz. Nauk* **178** 449 (2008) [*Phys. Usp.* **51** 427 (2008)]
23. Gulyaev Yu V, Barabanenkov Yu N, Barabanenkov M Yu, Nikitov S A *Phys. Lett. A* **335** 471 (2005)
24. Gulyaev Yu V, Barabanenkov Yu N, Barabanenkov M Yu, Nikitov S A *Phys. Rev. E* **72** 026602 (2005)
25. Barabanenkov M Yu, Barabanenkov Yu N, Gulyaev Yu V, Nikitov S A *Phys. Lett. A* **364** 421 (2007)
26. Barabanenkov Yu N, Barabanenkov M Yu *Elektromagnitnye Volny Elektron. Sistemy* (11) 16 (2007)
27. Vinogradov A P, Dorofeenko A V, Zouhdi S *Usp. Fiz. Nauk* **178** 511 (2008) [*Phys. Usp.* **51** 485 (2008)]
28. Ambartsumyan V A *Zh. Eksp. Teor. Fiz.* **13** 244 (1943)
29. Barabanenkov Yu N, Kouznetsov V L, Barabanenkov M Yu *Prog. Electromagn. Res., PIER* **24** 39 (1999)
30. Barabanenkov Y N, Barabanenkov M Y, in *PIERS 2006: Progress in Electromagnetics Research Symp., March 26–29, 2006, Cambridge, Mass., USA: Proc.* (Cambridge, Mass.: The Electromagnetics Academy, 2006) p. 10
31. Reid W *Indiana Univ. Math. J.* **8** 221 (1959)
32. Redheffer R *Indiana Univ. Math. J.* **8** 349 (1959)
33. Dorokhov O N *Pis'ma Zh. Eksp. Teor. Fiz.* **36** 259 (1982) [*JETP Lett.* **36** 318 (1982)]; *Solid State Commun.* **44** 915 (1982)
34. Mello P A, Pereyra P, Kumar N *Ann. Physics* **181** 290 (1988)
35. Klyatskin V I *Metod Pogruzheniya v Teorii Rasprostraneniya Voln* (Embedding Method in the Wave Propagation Theory) (Moscow: Nauka, 1986)
36. Barabanenkov Yu N, Kryukov D I *Waves Random Media* **2** (1) 1 (1992)
37. Mello P A, Stone A D *Phys. Rev. B* **44** 3559 (1991)
38. Yablonovitch E *Phys. Rev. Lett.* **58** 2059 (1987); John S *Phys. Rev. Lett.* **58** 2486 (1987)
39. Barabanenkov Yu N, Barabanenkov M Yu *Zh. Eksp. Teor. Fiz.* **123** 763 (2003) [*JETP* **96** 674 (2003)]
40. Barabanenkov Yu N, Kalinin M I *Phys. Lett. A* **163** 214 (1992)
41. Gazaryan Yu L *Zh. Eksp. Teor. Fiz.* **56** 1856 (1969) [*Sov. Phys. JETP* **29** 996 (1969)]
42. Anderson P W *Phys. Rev.* **109** 1492 (1958)
43. Gertsenshtein M E, Vasil'ev V V *Teor. Veroyatn. Ee Primen.* **4** 424 (1959) [*Theor. Probab. Appl.* **4** 391 (1959)]

PACS numbers: **41.20.-q**, **42.65.Pc**, **85.50.-n**
DOI: 10.3367/UFNe.0179.200905i.0539

Local fields in nanolattices of strongly interacting atoms: nanostrata, giant resonances, 'magic numbers,' and optical bistability

A E Kaplan, S N Volkov

S M Rytov took an interest in many things, including the theory of layered media with a period much smaller than the wavelength [*Zh. Eksp. Teor. Fiz.* **29** 605 (1955)]. One of us, A E K, who participated in Rytov's seminars for 20 years, until 1979, was also involved with multiple and various things, and was sometimes surprised to realize that his work touches upon old areas of interests of Rytov. Of course, there is little surprise here, because Rytov had an intuition for unusual and fundamental things, and he often looked far ahead. Our new results presented here echo, to an extent, those old interests of Rytov.

In this report, following our recent brief publication [1], we consider a number of new effects emerging in one- and two-dimensional ordered systems of two-level atoms with a sufficiently strong dipole interaction. We have shown that in systems smaller than the wavelength of light, an excitation of the atomic dipole moments may become substantially inhomogeneous, forming strata and two-dimensional structures of a nanometer scale. Such behavior of the local field in a dielectric system is significantly different from the results of the Lorentz–Lorenz theory for local fields; it gives rise to resonances defined by the size and geometry of the system and is capable of inducing a giant local-field enhancement. We demonstrated that the saturation nonlinearity in two-level atoms may cause optical bistability, in particular, in the simplest case where the system is comprised of two atoms only. We also predicted 'magic' system sizes and geometries that, unlike the Lorentz model, do not result in a suppression of the local field in the system when the laser frequency is tuned to the resonance of the two-level atom.

A known fact of the electrodynamics of continuous media is that the microscopic field acting on atoms or molecules (known as the 'local field') is generally different from the macroscopic (average) field because of the dipole interaction between the particles composing the medium. This difference is a central point of the classical theory of local fields in dielectrics advanced by Lorentz and Lorenz [2]. An important, albeit implicit, assumption of that theory is that the local field remains virtually unchanged from atom to atom over distances much shorter than the wavelength of light λ . The theory is therefore essentially based on the so-called 'mean-field approximation.'

Rapid advances in nanotechnology opened up possibilities of fabricating artificial systems of strongly interacting particles, for which the assumption of the local-field uniformity is no longer valid. It is natural to presume that abandoning the mean-field approximation in the description of the local fields may result in a discovery of many new and interesting phenomena, just as passing from the macroscopic Curie–Weiss theory to the Ising model significantly extended the ability of the theory to describe magnetic materials [3]. Of course, this does not mean that a complete analogy is to be expected in the descriptions of local fields and magnetic media. In our case, even more interesting discoveries can be expected because the atomic electric dipoles induced by the local fields are driven by an incident electromagnetic wave, in contrast to the static magnetic dipoles in the Ising model. Another crucial distinctive feature of our work is that the systems under consideration are very small, less than the wavelength in size, while the majority of studies in the theory of magnetism focus on building a macroscopic, ‘thermodynamic,’ description of the medium.

In this report, based on the results initially presented in our recent brief publication [1], we demonstrate that accounting for significant spatial variations of the local field from atom to atom, on a scale much less than the wavelength, opens the way for describing many new effects in ordered systems of strongly interacting atoms, including giant local-field resonances, ‘magic’ system sizes and geometries, and optical bistability and hysteresis. Of particular importance is that our research brings forward a totally new paradigm in the theory of light–matter interaction. Our calculations show that various field-related and array-related factors may disrupt a smooth variation of the local field from atom to atom, giving rise to nearly periodic strata or more complex patterns of induced dipole moments. They are most pronounced in one- and two-dimensional dielectric systems comprising atoms, molecules, quantum dots, clusters, or other resonant particles. The resonant nature of the interaction between the particles allows controlling the anisotropy and strength of the interaction. If the light wave then propagates normally to the one- or two-dimensional lattice, we can also eliminate wave propagation aspects of the problem.

In general, two major types of dipole strata emerge: short-wave, with the period up to four interatomic distances, and long-wave strata. The strata can be interpreted as standing waves of local-field excitations, which we hereafter call ‘locitons.’ The locitons are electrostatic by nature and can have a very low group velocity. They may be classified as Frenkel excitons [4] because the electrons are bound to the atoms and there is no charge transfer in the systems under consideration.

In the first approximation, the phenomenon under consideration is linear in the external field, and locitons can be excited within a spectral band much broader than the atomic linewidth. It essentially amounts to a Rabi broadening of a spectral line of a resonant atom, which arises because of strong interatomic interactions. The dipole strata can be controlled by adjusting the laser polarization and the dimensionless interatomic coupling parameter Q (see below), which depends, in turn, on the interatomic distance, on the dipole moment and spectral linewidth of the resonant transition in the atoms, and on the detuning of the laser frequency from the atomic resonance. For $|Q| > Q_{\text{cr}} = O(1)$, the smooth variation of the local field from atom to atom can

be broken by boundaries, impurities, defects in the lattice, etc. A most striking manifestation of the effect is the emergence of large local-field resonances due to lociton eigenmodes in finite arrays and lattices. Another interesting and unexpected phenomenon is an almost complete cancelation of the local-field suppression if the laser frequency is tuned exactly to the atomic resonance and the system is comprised of a certain ‘magic’ number of atoms. Moreover, in a system with a saturation nonlinearity, different types of optical bistability and hysteresis can emerge.

Our model is based on the dipole interaction between atoms. We can neglect retardation effects because of the small size of the system; therefore, similarly to the classical theory of local fields [2], we rely on the fact that the near field of a dipole is predominantly quasistatic and nonradiative in nature. The frequency ω of the incident laser radiation is close to the resonant frequency ω_0 of the atom, which we approximate by a two-level system [5–7] with a transition dipole moment d_a . The local field acting on an atom at a point \mathbf{r} can be represented as a sum of the field \mathbf{E}_{in} of the light wave incident on the system and the quasistatic contributions from all other dipoles (with their coordinates denoted as \mathbf{r}') that are induced by the local fields $\mathbf{E}_L(\mathbf{r}')$:

$$\mathbf{E}_L(\mathbf{r}) = \mathbf{E}_{\text{in}}(\mathbf{r}) - \frac{Q}{4} \sum_{\text{lattice}}^{\mathbf{r}' \neq \mathbf{r}} \frac{l_a^3}{|\mathbf{r}' - \mathbf{r}|^3} \times \frac{3\mathbf{u}[\mathbf{E}_L(\mathbf{r}') \cdot \mathbf{u}] - \mathbf{E}_L(\mathbf{r}')}{1 + |\mathbf{E}_L(\mathbf{r}')|^2/[E_{\text{sat}}^2(1 + \delta^2)]}, \quad (1)$$

where \mathbf{u} is the unit vector along $\mathbf{r} - \mathbf{r}'$, $\delta = T\Delta\omega = T(\omega - \omega_0)$ is the dimensionless detuning of the laser frequency from the atomic resonance, and $E_{\text{sat}}^2 = \hbar^2 \varepsilon / (|d_a|^2 \tau T)$ is the saturation intensity of the two-level system. The dimensionless coupling parameter

$$Q = \frac{4|d_a|^2 T}{\varepsilon \hbar l_a^3 (\delta + i)} \quad (2)$$

represents the strength of the dipole interaction between neighboring atoms. The coupling parameter and the saturation intensity depend on the transverse relaxation time $T = 2/\Gamma$ of the two-level atom, whose homogeneous spectral linewidth is Γ , on its longitudinal relaxation time (excitation life time) τ , and on the background dielectric constant ε . We also assume that the interatomic distance l_a is large enough to prevent any overlap between atomic orbitals of neighboring atoms, $l_a \gg |d_a|/e$. This assumption is, in fact, also present in the standard Lorentz theory of local fields [5–7], in which the interaction between atoms and molecules is treated classically. Our approach radically departs from the standard Lorentz theory in that we do not assume any averaging of the local field over the neighboring sites of the crystalline lattice, which would reveal itself in the assumption that $\mathbf{E}_L(\mathbf{r}) = \mathbf{E}_L(\mathbf{r}')$, and we do not use an encapsulating sphere around the observation point, outside which a continuous medium is assumed.

Large transition dipole moments, for example, in alkali vapors, CO_2 , narrow-band resonances in solids [9], quantum dots, and clusters may significantly enhance the effects that we discovered. In many of these cases, locitons can emerge with l_a as large as a few tens of nanometers. We note that surface plasmons in metal–dielectric composites [10, 11] usually require a more sophisticated theoretical description

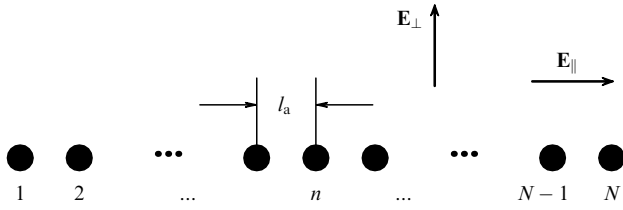


Figure 1. The geometry of the one-dimensional problem: the local field in an array of resonant atoms. The light wave propagates normally to the plane of the picture.

involving long-range dipole interactions, and hence that case falls outside the scope of our report.

We first consider a simpler problem of finding the local field in a one-dimensional array of atoms arranged along the z axis with equal interatomic distances l_a (Fig. 1). A laser beam, which is incident normally to the array, is polarized either along the array ($\mathbf{E}_{\text{in}} \parallel \hat{\mathbf{e}}_z$), thus inducing atomic dipole moments that are parallel to the array axis, or perpendicular to the array ($\mathbf{E}_{\text{in}} \perp \hat{\mathbf{e}}_z$), accordingly aligning the dipoles normally to the array and parallel to each other. In both cases, we have $\mathbf{E}_L \parallel \mathbf{E}_{\text{in}}$, and hence the equations for the field are reduced to scalar ones. Using the dimensionless variables $\mathcal{E}_n = [E_L(\mathbf{r}_n)/E_{\text{in}}]_{(p)}$, where $(p) = \parallel, \perp$ denotes the field polarization, we can write Eqn (1) for each polarization as

$$\mathcal{E}_n - \frac{\delta_R}{2(\delta + i)} \sum_{\text{chain}}^{j \neq n} \frac{\mathcal{E}_j/S}{|j - n|^3} = 1, \quad (3)$$

where $1 \leq n, j \leq N$,

$$\delta_R = -4SF_{(p)} \frac{|d_a|^2 T}{\epsilon \hbar l_a^3}, \quad (4)$$

and the summation in Eqn (3) is performed over all atoms in the one-dimensional array (chain), resulting in the appearance of the factor $S = \sum_{j=1}^{\infty} j^{-3} \approx 1.202$. The factor $F_{(p)}$ is defined by the field polarization, $F_{\parallel} = 1$ and $F_{\perp} = -1/2$. In the nearest-neighbor approximation, similarly to the Ising model for magnetic media, the summation over all atoms in Eqn (3) may be replaced with a simpler sum, $\mathcal{E}_{n-1} + \mathcal{E}_{n+1}$ (one can then set $S = 1$). In both cases [i.e., for the full summation in Eqn (3) and in the nearest-neighbor approximation], the results are qualitatively similar. In the case of a two-atom system, discussed below, the two approaches naturally merge.

As $N \rightarrow \infty$, a solution of Eqn (3) can be found as a sum of the uniform ‘Lorentz’ field

$$\bar{\mathcal{E}} = \frac{\delta + i}{\delta - \delta_R + i}, \quad (5)$$

and wave contributions of the form $\Delta \mathcal{E} \propto \exp(\pm iqn)$. The wave number of each of these spatially oscillating solutions is $q = 2\pi l_a/\Lambda$, and the wavelength Λ , to be found later, is usually much shorter than the wavelength of the incident light. Here, we note an analogy to the phonon theory [4], except that our case involves not mechanical vibrations of atomic nuclei but excitations of bound electrons. The solution of Eqn (3) is very anisotropic, with a pronounced dependence on the polarization of the incident wave. The homogeneous ‘Lorentz’ component of the local field is significantly suppressed at the exact resonance, i.e., if the laser frequency is tuned to the frequency of the atomic transition, $\delta = 0$, and

the dipole interaction between atoms is strong, $|\delta_R| \gg 1$:

$$|\bar{\mathcal{E}}_{\text{res}}|^2 = \frac{1}{1 + \delta_R^2} \ll 1. \quad (6)$$

In this case, the field is essentially pushed out from the system. $|\bar{\mathcal{E}}|$ reaches its maximum at $\delta = \delta_R$,

$$|\bar{\mathcal{E}}_{\text{peak}}|^2 = 1 + \delta_R^2 \gg 1. \quad (7)$$

The wave vectors q are found from the dispersion relation

$$\frac{1}{S} \sum_{n=1}^{\infty} \frac{\cos(nq)}{n^3} = \frac{\delta + i}{\delta_R}. \quad (8)$$

(In the nearest-neighbor approximation, the entire left-hand side of this equation may be replaced with $\cos q$.)

Within our present model, we showed that spatially oscillating solutions emerge if $|\delta_R| > 1$ in the range of frequency detunings $1 > \delta/\delta_R > -3/4$. (In the nearest-neighbor approximation, this range widens: $|\delta/\delta_R| < 1$.) The dipole strata are especially pronounced for $|\delta_R| \gg 1$. The strength of the dipole interaction between atoms may be gauged by the Rabi frequency $\Omega_R = \delta_R/T$, which essentially defines the position of the Lorentz resonance with respect to the atomic transition frequency. The Rabi frequency sets the width of the energy-spectrum band where locsitos can exist, such that for $|\delta_R| \gg 1$, this width is $\sim 2\hbar|\Omega_R| \approx \hbar\Gamma$. Here, we may draw some analogies with energy spectrum bands in solids [4] and in photonic crystals [12]. In the limit $1 - \delta/\delta_R \ll 1$ (i.e., on the band edge near the Lorentz resonance, where $\delta \approx \delta_R$), ‘long-wave’ locsitos emerge, with

$$q_{\text{LW}} \approx \sqrt{1 - \frac{\delta^2}{\delta_R^2}}, \quad (9a)$$

$$\Lambda_{\text{LW}} = \frac{2\pi l_a}{q_{\text{LW}}}. \quad (9b)$$

It is worth noting that their wavelength Λ_{LW} may be as large as $2\pi l_a \delta_R$, while remaining much shorter than the wavelength of the incident light wave. A typical example of such strata is presented in Fig. 2 (top curve). At the opposite edge of the locsiton frequency band (in the nearest-neighbor approximation, it corresponds to $1 + \delta/\delta_R \ll 1$), short-wave locsitos emerge with $q_{\text{SW}} \lesssim \pi$ and $\Lambda_{\text{SW}}/2 \gtrsim l_a$, which is close to the shortest spatial oscillation wavelength possible in a discrete system.

Because $\Lambda_{\text{SW}}/2$ is generally not a multiple of l_a , the distribution of dipole moments and the corresponding local fields in the discrete array of atoms may be spatially modulated with a longer wavelength, much like in the case of two waves with close wave vectors. Such modulation is clearly visible in the middle curve in Fig. 2, where $\Lambda_{\text{SW}}/2$ is quite close to l_a . The case of the exact resonance of the incident wave with the atomic transition, for which $\delta = 0$, may be used to divide the locsiton frequency band into the regions with short-wave and long-wave locsitos. The boundary case, with $\Lambda = 4l_a$, is represented by the lower curve in Fig. 2.

To draw an analogy with phonons, we note that long-wave locsitos are counterparts of acoustic phonons, and short-wave locsitos correspond to optical phonons. Another interesting analogy can be drawn with ferromagnetic or

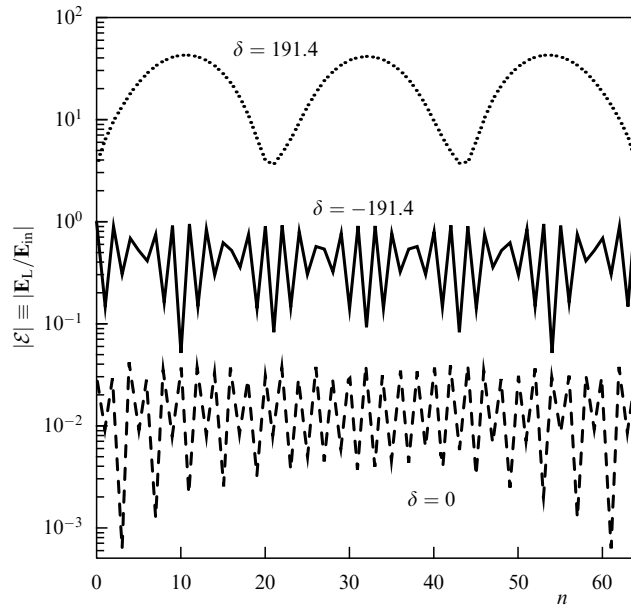


Figure 2. Dipole strata in an array of $N = 65$ atoms: the distribution of the absolute value of the local field at $\delta_R = 200$ at three different laser frequency detunings δ ; n is a sequential number of an atom in the array.

ferroelectric materials, which feature strong interaction between static magnetic or electric dipoles. Within this analogy, the locsitons with the longest wavelengths resemble ferromagnets, while those with the shortest wavelengths resemble antiferromagnets. A similar analogy may also be noticed in the difference between bistability regimes in these two extreme cases, which we consider below for the simplest, two-atom, system.

We emphasize that this analogy between the locsitons and ferromagnets or ferroelectrics is inevitably very limited. For example, at $\delta = 0$, a hybrid configuration of a sort is formed by the induced atomic dipoles in the array, $\uparrow \circ \downarrow \circ \uparrow \dots$, which corresponds to the lower curve in Fig. 2. Such hybrid configurations are only possible because of the dynamic nature of the atomic dipoles in our optical problem, and are unattainable with static dipoles. Thus, the dipole configuration in an array of atoms can be smoothly transformed from a ‘ferromagnetic-like’ to an ‘antiferromagnetic-like’ by tuning the laser frequency from one locsiton band edge to the other, while going through all the different hybrid configurations in the process.

We have shown that a finite array of atoms should exhibit size-related resonances, which are somewhat similar to resonances in thin semimetal films [13], long organic molecules [14], or a common violin string. The main difference is that in our case, the number of resonances is limited by the number of atoms N . The linear system of equations (3) may be solved, for example, by using numerical matrix solvers for $N \gg 1$, while for small N , the problem is amenable to analytic methods. Some results for the local field E_L obtained using numerical methods are shown in Figs 2–5.

We also used the following simple approximation to achieve a better qualitative understanding of the numerical results. The solution for an infinite array of atoms can be used to approximate the solution for a finite array of N atoms as a sum of the uniform ‘Lorentz’ solution \bar{E} at $N = \infty$ and spatially oscillating components $\Delta E \propto \exp(\pm iqn)$, where the resonant locsiton wavenumber q and the resonant amplitude

ΔE are found from appropriate boundary conditions for the local field at the array ends. If the interaction between all atoms is taken into account, boundary conditions can only be approximated; however, we verified the precision of such an approximation for locsitons with sufficiently long wavelengths by many numerical simulations.

In the nearest-neighbor approximation, the method described above yields an exact solution of the problem. In this solution, the half-wavelength $\Lambda_1/2 = (N+1)l_a$ of the resonant locsiton with the longest wavelength is determined from the condition that the nodes of the local-field eigenmode lie beyond the end atoms of the array at the distances l_a , i.e., $E_0 = E_{N+1} = 0$. The frequency resonances for the locsitons are defined by the frequency detuning δ_k ($0 < k \leq N$):

$$\delta_k = \delta_R \cos qk, \quad (10a)$$

where

$$qk = \frac{\pi k}{N+1}. \quad (10b)$$

The corresponding locsiton wavelength is $\Lambda_k = \Lambda_1/k$. Due to symmetry considerations, only resonances with an odd k may be excited by an incident laser beam with a symmetric transverse field profile, while resonances with an even k may be excited by a beam with an antisymmetric profile. The solid curve in Fig. 3 depicts resonances of the maximum local field

$$E_{\max} \equiv \max_{0 < n \leq N} |E_n|$$

at the atoms in the array; the resonances are obtained in the nearest-neighbor approximation for a uniform distribution of the incident field along an array with $N = 13$ and $\delta_R = 200$. The lower envelope for this curve is $E_{\text{low}}(\delta) \approx 2\bar{E}$, while the

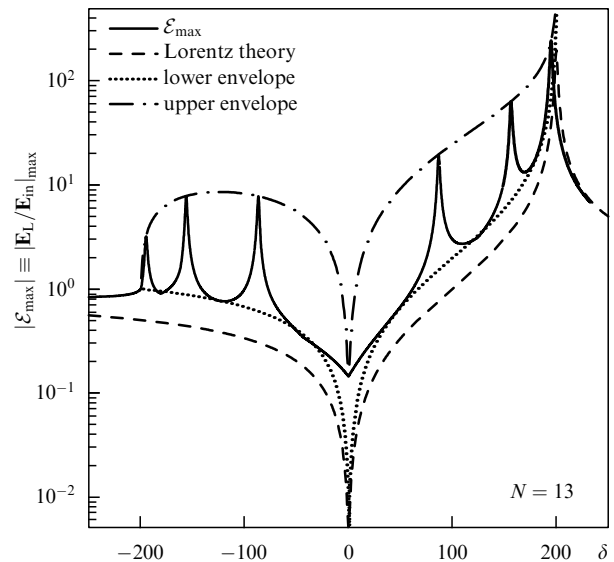


Figure 3. Locsiton resonances appearing in the dependence of the normalized maximum amplitude E_{\max} of the local field on the laser frequency detuning δ in an array of $N = 13$ atoms with $\delta_R = 200$ (solid curve). For comparison, its upper and lower envelopes are shown, along with the corresponding dependence obtained using the classical Lorentz theory for unbounded media (the dashed curve).

upper envelope, obtained in the nearest-neighbor approximation, is given by

$$\mathcal{E}_{\text{up}} \approx \begin{cases} \bar{\mathcal{E}} \left(n_{\delta} + \frac{1}{n_{\delta}} \right), & n_{\delta} \leq 1, \\ 2\bar{\mathcal{E}}, & n_{\delta} > 1, \end{cases} \quad (11a)$$

where

$$n_{\delta} = \frac{N+1}{2\sqrt{\delta_R^2 - \delta^2}}. \quad (11b)$$

As N increases, the resonances start merging and become weaker as N approaches δ_R . However, even for large N , the lower envelope \mathcal{E}_{low} is still twice the local field $\bar{\mathcal{E}}$ predicted by the classical Lorentz theory [see Eqn (5)].

For $N = 3k - 1$, where k is a natural number, the local-field amplitude \mathcal{E}_{max} , which is obtained in the nearest-neighbor approximation, goes below \mathcal{E}_{low} at $\delta = -\delta_R/2$. For this frequency detuning δ , the absolute value of the locsiton wave number is $|q| \approx 2\pi/3$, and the spatial period of the locsiton is $A = 3l_a$. The long-wavelength modulations of the spatial profiles of the dipole moments and the local field in the array disappear in this case because A becomes an integer multiple of l_a . This results in an ‘antiresonance’ of a sort appearing in the dependence of the local field \mathcal{E}_{max} on δ ; in other words, the locsiton in the array becomes suppressed.

Another important and unusual effect that we discovered is the cancelation of the resonant local-field suppression in an array consisting of a certain ‘magic’ number of atoms. At the exact resonance of laser radiation with the atomic transition (i.e., at $\delta = 0$) and for $|\delta_R| \gg 1$, the local field obtained from the Lorentz theory is ‘pushed out’ of the system [see Eqn (6)]. We call this effect the resonant local-field suppression; it is also present in finite arrays of atoms for most N . We found, however, that at a certain magic number N , this resonant suppression vanishes, and the local field penetrates the system even at $\delta = 0$. In the nearest-neighbor approximation, the magic array sizes are $N = km_{\text{mag}} + 1$, where k is a natural number and $m_{\text{mag}} = 4$. The effect is most pronounced at $N = 5$, where the atomic dipoles arrange as $\uparrow \circ \downarrow \circ \uparrow$, with the amplitudes of the dipoles and the local field reaching their maxima ($\mathcal{E}_{\text{mag}} \approx 1/3$) at odd-numbered atoms, while almost vanishing at even-numbered atoms. The ‘magic enhancement’ of the local field (compared to the uniform, Lorentz case) can be substantial: $|\mathcal{E}_{\text{mag}}/\bar{\mathcal{E}}_{\text{res}}| \approx \delta_R/3$. In this effect, one of the resonant locsitons, whose frequency exactly matches that of the atomic transition, virtually compensates the resonant suppression of the local field in the system. The effect is also present if interactions between all atoms in the array are taken into account [see Eqn (3)], where $m_{\text{mag}} = 13$. While an interference of an evil spirit cannot be excluded completely, we assume that the result stems from properties of the equation for the wave vector q of a locsiton in the array of atoms; this equation follows from Eqn (8) at $\delta = 0$:

$$\sum_{n=1}^{\infty} \frac{\cos(nq)}{n^3} = 0. \quad (12)$$

The smallest positive root q_1 of Eqn (12) is such that q_1/π is very close to a rational number, $(q_1/\pi)/(6/13) = 1.00026\dots$, and hence the locsiton wavelength is $A = 2\pi/q_1 \approx (13/3)l_a$, and a multiple of $A/2$ is therefore close to a multiple of l_a . Therefore, the resonant local-field suppression is canceled at

$N = 14$, with the relative amplitude of the field becoming substantial, $\mathcal{E}_{\text{mag}} \approx 2/15$.

There is a semantic irony in that the local-field effects are actually due to nonlocal interactions between atoms. If the field of an incident wave is limited to a small spatial region, the local field can extend beyond this region; locsitons can propagate away from their origin. At the edges of the locsiton frequency band, i.e., at $|\delta_R| > |\delta| \gg 1$, the group velocity of a locsiton $v_{\text{gr}} \approx l_a(\Omega_R^2 - \Delta\omega^2)^{1/2}$ could be lower than the speed of sound in a solid. This effect can be useful, for instance, in designing nanometer-scale delay lines that could be used in molecular computers or integrated nanodevices for optical signal processing.

Aside from dipole strata, other even more interesting structures emerge in two-dimensional lattices of resonant atoms. For example, we consider a standing electromagnetic wave acting on an equilateral triangular lattice of atoms, the wave being polarized perpendicular to the lattice plane. The interatomic distances are very small, of the order of a few nanometers, and hence the external field can be regarded as uniform on a scale of several tens or even several hundred of atoms. We found that at certain conditions, concentric dipole strata (Fig. 4) can emerge around a circular hole made by removing several tens of atoms from the lattice; the amplitude of the strata decreases fast as the distance to the hole boundary increases. An even more interesting dipole configuration emerges if the laser radiation is incident normally to the lattice and polarized in the lattice plane. For better qualitative understanding of the local-field behavior in this case, we use the ‘near-ring approximation,’ which is a modification of the nearest-neighbor approximation: we consider interactions of each atom with its six immediate neighbors only, while assuming that the positions of the six atoms are evenly ‘spread’ over a circle with the diameter of one interatomic distance l_a . As in the one-dimensional case, we introduce a polarization-independent dimensionless parameter $\tilde{\delta}_R$, which differs from δ_R defined by Eqn (4) in that we set $SF_{(p)} = -1$ here:

$$\tilde{\delta}_R = \frac{|d_a|^2 T}{\epsilon \hbar l_a^3}. \quad (13)$$

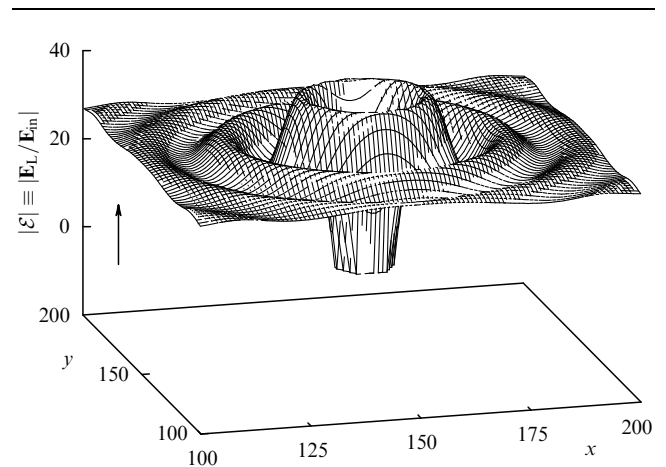


Figure 4. Localization of a locsiton in a two-dimensional triangular lattice of atoms around a hole with a diameter of 15 interatomic distances. The distribution of the local field \mathcal{E} in the system is shown in the case where the external field of the light wave is normal to the lattice plane, $\delta = 100$, and $\tilde{\delta}_R = 69$.

Comparing Eqns (2) and (4), we see that $Q = \tilde{\delta}_R/(\delta + i)$. After replacing the summation in Eqn (1) by an integration over the ‘near ring’ described above, we find a simple isotropic expression for the uniform Lorentz local field:

$$\bar{\mathbf{E}}_L = \frac{\mathbf{E}_{in}}{1 + (3/4)Q}. \quad (14)$$

It can be demonstrated that Eqn (14) remains valid not only in the near-ring approximation but also in the context of more precise calculations, which account for the structure of the two-dimensional lattice of atoms and for the dependence of the solution on the direction of the locsiton wave vector \mathbf{q} within the first Brillouin zone. As in the one-dimensional case, we sought a solution of Eqn (1) as a superposition of the Lorentz field $\bar{\mathbf{E}}_L$ and plane-wave locsitons with the coordinate dependences $\exp(\pm i\mathbf{q}\mathbf{r}/l_a)$. Assuming that \mathbf{q} makes an angle ψ with the polarization direction of the incident laser radiation, we arrive at the following dispersion relation for two-dimensional locsitons (which is a good approximation for relatively long-wavelength locsitons):

$$1 + \frac{3}{4}Q[J_0(q) - 3J_2(q)\cos(2\psi)] = 0, \quad (15)$$

where J_n is a Bessel function of the first kind.

The near-ring approximation becomes insufficient for short-wavelength locsitons; a more detailed study is required in this case, which takes account of the symmetry of the triangular lattice of atoms and the respective Brillouin zone structure. We have shown that the solution in this more general case depends on the orientation of the incident laser polarization with respect to the lattice. We let \mathbf{u}_K denote the unit vector pointing from a given atom to one of its nearest neighbors (this corresponds to the ΓK direction in the first Brillouin zone). We consider four most interesting configurations defined by different polarizations and orientations of the locsiton wave vector:

- a) $\mathbf{q} \perp \mathbf{E}_{in}, \quad \mathbf{E}_{in} \parallel \mathbf{u}_K,$
- b) $\mathbf{q} \perp \mathbf{E}_{in}, \quad \mathbf{E}_{in} \perp \mathbf{u}_K,$
- c) $\mathbf{q} \parallel \mathbf{E}_{in}, \quad \mathbf{E}_{in} \parallel \mathbf{u}_K,$
- d) $\mathbf{q} \parallel \mathbf{E}_{in}, \quad \mathbf{E}_{in} \perp \mathbf{u}_K.$

The respective dispersion relations in these four cases are found by us to be

- a) $\cos \frac{q\sqrt{3}}{2} = 4(1 + Q^{-1}),$
- b) $\cos \frac{q}{2} = \frac{1}{8} \left[5 \pm \sqrt{57 + 64Q^{-1}} \right],$
- c) $\cos \frac{q}{2} = \frac{1}{16} \left[1 \pm \sqrt{1 + 128(1 - Q^{-1})} \right],$
- d) $\cos \frac{q\sqrt{3}}{2} = \frac{2}{5}(1 - 2Q^{-1}).$

The dipoles induced in a finite two-dimensional lattice form distinctive patterns if locsiton resonances emerge at the same Q in both dimensions. In the limit of long-wavelength locsitons ($q \ll 1$), the dispersion relations in cases (a) and (b) coincide with each other and with the result obtained in the near-ring approximation [see Eqn (15)]. In these two cases,

$\psi = \pi/2$ and $Q \approx -4/3$, while

$$q_a^2 \approx q_b^2 \approx q_{ring}^2 \approx -\frac{32}{3} \left(\frac{3}{4} + \frac{1}{Q} \right). \quad (16)$$

In a similar manner, we obtain approximate solutions in cases (c) and (d), for which $\psi = 0$:

$$q_c^3 \approx q_d^3 \approx q_{ring}^2 \approx \frac{32}{15} \left(\frac{3}{4} + \frac{1}{Q} \right). \quad (17)$$

Combining cases (a) and (b) or cases (c) and (d), we can achieve simultaneous resonances in both directions in the lattice, if the lattice is approximately square in shape. Resonances of the same order are attained this way for locsitons with wave vectors pointing in two orthogonal directions; a sufficient ‘squareness’ of the two-dimensional triangular lattice can be achieved by choosing the lattice size (i.e., the numbers of atoms in the two directions). Locsitons with shorter wavelengths and wave vectors pointing in different directions are also present, but they do not significantly affect the emerging dipole pattern because of their nonresonant nature.

The interference of locsitons in a two-dimensional lattice of atoms can produce many different dipole excitation patterns and strata. Some of them are reminiscent of ‘quantum carpets’ [15]. Figure 5 depicts vector patterns that are formed by the atomic dipoles induced by the local field. The atoms are arranged in a 48×56 equilateral triangular lattice, which results in approximately equal sides of the lattice patch. The field of the incident electromagnetic wave is uniform and is polarized along the diagonal of the lattice patch. The incident wave frequency is chosen such that the third resonance (in the order of increasing wavenumbers, counting only the resonances allowed by the symmetry of the problem) is excited in each dimension; at least six distinct vortices of the local field are visible. Figure 5 shows the

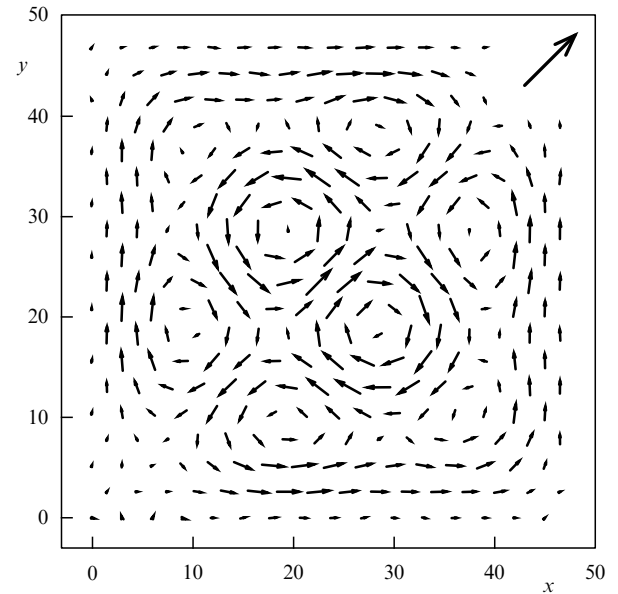


Figure 5. Vortices in the distribution of the local field \mathcal{E} in a nearly square patch of a two-dimensional triangular lattice of atoms at $\delta = -1000$ and $\tilde{\delta}_R = 1316.5$. To avoid overcrowding of the plot, only one of each nine dipoles is shown. The incident light wave is polarized in the lattice plane along the diagonal of the lattice patch, its field shown by the large arrow.

imaginary parts of the complex field amplitudes, because they are dominant for each of the resonant locitons.

Finite two-dimensional lattices and other similar systems of resonant atoms produce especially interesting examples of the cancelation of the resonant local-field suppression. Unlike in the one-dimensional arrays of atoms, the ‘restoration’ of the local field in such systems at $\delta = 0$, compared to that in the uniform, Lorentz case, can be more complete (up to 100%). The two-dimensional ‘magic shapes’ of atoms have the same ‘cabbalistic’ streak as in the one-dimensional case. For example, in the nearest-neighbor approximation, the effect is most pronounced only in the system of $N = 13$ atoms arranged as an equilateral six-point star with an atom at the center, for which the maximum restoration of the local field is reached, $\mathcal{E}_{\max} \approx 1.02$. The directions and relative amplitudes of the local field at the atoms in this system are shown in Fig. 6 for $\mathbf{E}_{\text{in}} \parallel \mathbf{u}_K$. It can be seen from the picture that the local field is concentrated on the outermost atoms and the one at the center, while the local field at the inner hexagon of atoms is almost completely suppressed. Any symmetry distortion in this system of strongly interacting atoms (e.g., by attaching a foreign atom or molecule to it) would break the balance of the local fields in the system and bring back the resonant suppression of the local field, which is canceled in the symmetric ‘magic system.’ This effect may be used, inter alia, in designing nanometer-scale sensors for detecting various biological molecules.

A sufficiently strong electromagnetic field applied to a system of strongly interacting atoms can bring about nonlinear local-field effects, e.g., solitons. A detailed consideration of many and varied interesting effects of this kind falls out of the scope of this report. It is worth noting, however, that some nonlinear effects, such as optical bistability and hysteresis, are possible even in the steady-state regime considered here, where the amplitude of the incident electromagnetic wave is constant. The optical bistability for the uniform, Lorentz local field in an unbounded medium was predicted in [16] and experimentally observed later in [17]. However, the possibility of bistability and multistability for short-wavelength locitons, whose local field is highly nonuniform in space, has not been discussed in the literature. We found that this effect is possible even in the ultimately simple system of two two-level atoms with a saturation nonlinearity and a strong dipole interaction. This system also provides the most dramatic example of a self-induced local-field nonuniformity.

We describe the two-atom system using Eqns (3) and (4) with $S = 1$. Depending on the orientation of the local and

external fields $\mathbf{E}_L \parallel \mathbf{E}_{\text{in}}$ either perpendicular or parallel to the line connecting the two atoms, Eqn (4) respectively includes either F_{\perp} or F_{\parallel} . We introduce dimensionless amplitudes of the local field at each atom, $Y_j = E_j/E_{\text{sat}}$, where $j = 1, 2$, and the dimensionless field of the incident wave, $X = E_{\text{in}}/E_{\text{sat}}$, by normalizing the amplitudes of these fields to the saturation field E_{sat} of the two-level system. With this new notation, the system of equations for the local fields takes the form

$$Y_1 = X + \frac{\delta_{R2}(\delta - i) Y_2}{1 + \delta^2 + |Y_2|^2}, \quad (18a)$$

$$Y_2 = X + \frac{\delta_{R2}(\delta - i) Y_1}{1 + \delta^2 + |Y_1|^2}, \quad (18b)$$

where $\delta_{R2} \equiv \delta_R/2 > 0$. Equations (18) give rise to two types of solutions, or two different modes, for the local field in the system. A solution of the first type is similar to the uniform Lorentz solution for an infinite array of atoms, in which the local fields at the two atoms oscillate in phase. In this case, system of equations (18) leads to a cubic equation for $|\bar{Y}|^2$, which is readily solved or analyzed with the help of a plot, Fig. 7. For $|\delta_{R2}| \gg 1$, the onset of bistability and hysteresis for \bar{Y} occurs at the detuning $\delta \approx \delta_{R2}$ of the laser frequency from the frequency of the two-level transition, with $\delta_{R2} - \delta > \sqrt{3}$. In this case, the threshold field of the incident wave $X_{\text{thr}} \approx [(2/\sqrt{3})^3/\delta_{R2}]^{1/2} \ll 1$, i.e., it may be significantly below the saturation field E_{sat} of the two-level system.

In the case of antiphase oscillations of local fields, a multistable solution of the second type is in fact the limit case of a short-wave lociton that emerges at the opposite edge of the lociton band at $\delta \approx -\delta_{R2}$. In the limit $|X| \ll \delta_{R2}$, in addition to the uniform, Lorentz local field $\bar{Y} \approx X/2$, we found a nonuniform solution

$$Y_{1,2} = \bar{Y} \pm s, \quad (19a)$$

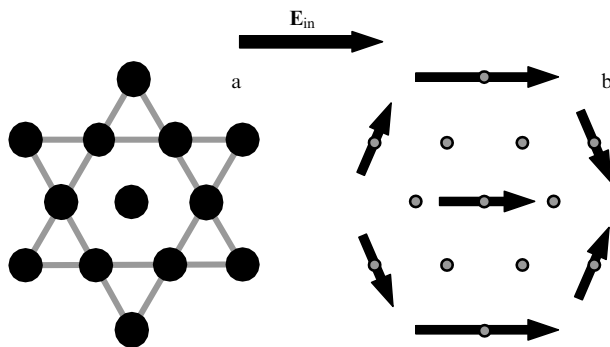


Figure 6. (a) The geometry of a ‘magic system’ of 13 resonant atoms; (b) the local field distribution in the system.

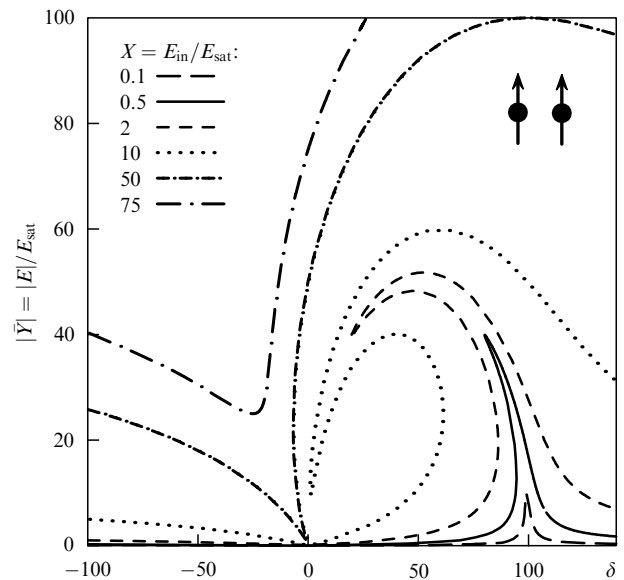


Figure 7. Optical bistability and hysteresis in a system of two resonant atoms with the saturation nonlinearity. The dependences of the normalized local-field amplitude $|\bar{Y}|$ on the frequency detuning δ are shown for $\delta_{R2} = 100$ and different normalized field amplitudes X of the incident wave.

where

$$s = \frac{\sigma}{\sqrt{2}} \left(\sqrt{1 \mp R} - i \sqrt{1 \pm R} \right), \quad (19b)$$

$$\sigma = \sqrt{\delta_{R2}(\delta_{R2} + \delta) - 2\bar{Y}^2 \pm \bar{Y}^2 R}, \quad (19c)$$

$$R = \sqrt{1 - \frac{\delta_{R2}^2}{\bar{Y}^4}}. \quad (19d)$$

The choice of the signs in Eqns (19b) and (19c) is independent of the choice of the sign in Eqn (19a). In Eqn (19a), one of the possible choices for the \pm sign corresponds to Y_1 and the other corresponds to Y_2 , which enables two different solutions, depending on the signs chosen. A similar property leads to the split-fork bistability for counterpropagating waves in a ring resonator [18]. The necessary conditions for the second-type multistable solution for the local field are $\delta_{R2} + \delta > \sqrt{3}$ and $X^2 > 4\delta_{R2}$. Three branches of the solution are seen in Fig. 8 near the bistability threshold: two stable branches given by Eqns (19) and one unstable ‘Lorentz’ solution \bar{Y} . For $\delta_{R2} + \delta > 2$, there exist five different branches of the solution, but only two of them are stable. The antiphase oscillations of the dipole moments of the two atoms, which are represented by the term $\pm s$ in Eqn (19a), could be likened to a pair of spins one of which is aligned and the other counter-aligned with the applied magnetic field.

Returning to the above-mentioned similarities between the local-field behavior in a system of atoms and the behavior of spins in magnetic materials, we emphasize that our research is focused on the effects that are characteristic of fairly small systems of atoms, while studies of magnetic phenomena are typically aimed at finding averaged, ‘thermo-

dynamic’ properties of sufficiently large systems. It is possible that our approach, which allowed us to predict giant resonances, magic numbers and shapes of atoms, etc., may allow exposing similar effects in nanometer-scale magnetic systems. The internal structure of locitons and dipole strata emerges at the nanometer scale, with many interesting effects involving drastic changes of the local field even between neighboring atoms, i.e., at distances of the order of a few nanometers or less. Optical methods are ill-suited for resolving such small systems, and therefore the X-ray or electron-energy-loss spectroscopies, as well as an observation of the size-related optical resonances predicted by us, may become more promising methods for detecting locitons experimentally.

We note that locitons and dipole nanostrata may open up fresh opportunities in designing elements for molecular computers and other nanodevices [19]. The significant advantage of locitons over electrons in semiconductors and metals is that no electric current or charge transfer is required for locitons to emerge. This advantage might aid in reducing the sizes of computer logic elements, since current semiconductor technology suffers from heat-related problems on a scale below 10 nm.

Locitons might be put into service in both passive elements (e.g., for data transmission or in delay lines) and active elements (switches or logic elements). Lociton-based nanodevices could thus supplement the list of alternative nanotechnologies, including plasmonics [20, 21], which is substantially based on surface plasmons [10, 11], and spintronics [22]. Another application of locitons could be in nanosensors for biological molecules and other particles and impurities. Such a nanosensor may be built out of resonant receptor molecules, which can selectively bind target molecules or particles; otherwise, receptor molecules may be attached to particles with an optical resonance. By arranging the molecules in a magic shape, the nanosensor may be designed such that the lociton in the system is not suppressed even at the exact resonance of the laser radiation with the constituent molecules; at the same time, the lociton is to be suppressed whenever a target biological molecule attaches to the nanosensor.

Even more exciting opportunities open up in arrays and lattices of atoms with an inverse population of the resonant quantum transition; this inverse population may be created by an appropriate (e.g., optical) pumping. Such systems may open up the way to controlling locitons, amplifying them, and even generating coherent locitons with a ‘lociton laser’ of a sort (a ‘locster’).

In conclusion, we demonstrated that dipole nanostrata and short-wave excitations of a local field (locitons) can be brought about in arrays and lattices of strongly interacting atoms, including a two-atom system, by the action of laser radiation with a frequency close to that of the atomic resonance. Locitonic effects include giant size-related resonances of the local field, the cancelation of the resonant local-field suppression in the system at certain magic shapes and numbers of atoms, and also optical bistability and hysteresis.

The authors are grateful to the US Air Force Office of Scientific Research (AFOSR) for funding this research.

References

1. Kaplan A E, Volkov S N *Phys. Rev. Lett.* **101** 133902 (2008)

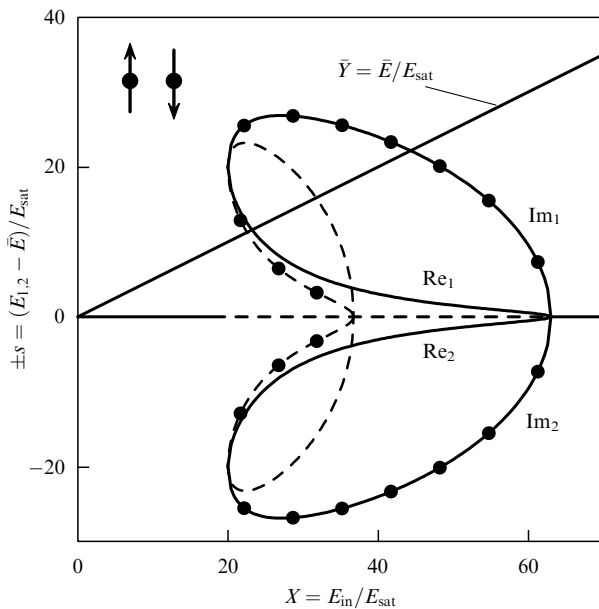


Figure 8. Optical bistability in the system of two resonant atoms with a saturation nonlinearity at $\delta_{R2} = 100$ and $\delta_{R2} + \delta = 10$. The thicker solid line represents the average uniform (‘Lorentz’) solution. The curves show the dependences of the ‘nonuniform components’ of our solution on the normalized field amplitude X of the incident wave. The solid and dashed curves respectively correspond to the stable and unstable regimes; the real parts of the solutions are shown with the curves marked with black dots, the imaginary parts are shown with the unmarked curves.

2. Born M, Wolf E *Principles of Optics* 6th ed. (Oxford: Pergamon Press, 1980), (Chapter 2 and the references therein) [Translated into Russian: 2nd ed. (Moscow: Nauka, 1973)]
3. Aharoni A *Introduction to the Theory of Ferromagnetism* 2nd ed. (Oxford: Oxford Univ. Press, 2000)
4. Kittel Ch *Introduction to Solid State Physics* 7th ed. (New York: Wiley, 1996) [Translated into Russian (Moscow: Nauka, 1978)]
5. Bowden C M, Dowling J P *Phys. Rev. A* **47** 1247 (1993)
6. Maki J J et al. *Phys. Rev. Lett.* **67** 972 (1991)
7. Butylkin V S, Kaplan A E, Khronopulo Yu G *Zh. Eksp. Teor. Fiz.* **59** 921 (1970) [*Sov. Phys. JETP* **32** 501 (1971)]
8. Landau L D, Lifshitz E M *Teoriya Polya* (The Classical Theory of Fields) (Moscow: Nauka, 1988) [Translated into English (Oxford: Butterworth-Heinemann, 1980)]
9. Steel D G, Rand S C *Phys. Rev. Lett.* **55** 2285 (1985)
10. Shalaev V M et al. *Opt. Lett.* **30** 3356 (2005)
11. Markel V A, Sarychev A K *Phys. Rev. B* **75** 085426 (2007)
12. Yablonovitch E *Phys. Rev. Lett.* **58** 2059 (1987)
13. Sandomirskii V B *Zh. Eksp. Teor. Fiz.* **52** 158 (1967) [*Sov. Phys. JETP* **25** 101 (1967)]
14. Chernyak V, Volkov S N, Mukamel S *Phys. Rev. Lett.* **86** 995 (2001)
15. Kaplan A E et al. *Phys. Rev. A* **61** 032101 (2000)
16. Bowden C M, Sung C C *Phys. Rev. A* **19** 2392 (1979)
17. Hehlen M P et al. *Phys. Rev. Lett.* **73** 1103 (1994)
18. Kaplan A E, Meystre P *Opt. Commun.* **40** 229 (1982)
19. Heath J R, Ratner M A *Phys. Today* **56** (5) 43 (2003)
20. Murray W A, Barnes W L *Adv. Mater.* **19** 3771 (2007)
21. Fainman Y et al. *Opt. Photon. News* **17** (7) 24 (2006)
22. Žutić I, Fabian J, Das Sarma S *Rev. Mod. Phys.* **76** 323 (2004)

PACS numbers: **05.40. – a**, **05.45. – a**, 42.25.Dd, **46.65. + g**, 47.27.eb
DOI: 10.3367/UFNe.0179.200905j.0547

Modern methods for the statistical description of dynamical stochastic systems

V I Klyatskin

1. Introduction

S M Rytov gave much attention to the development of functional methods of stochastic system analysis at All-Moscow Radiophysics Seminars he led. He dubbed them *radiomathematics*. I participated in these seminars from the end of the 1960s. S M Rytov frequently asked, me in particular, a question: “What are you studying?” I traditionally answered that solutions of stochastic equations (ordinary and partial differential, or integral) are functionals from random coefficients of these equations and that I am studying the dependence of the statistical characteristics of these solutions on various models and the statistical parameters of these coefficients. For about 30 years I considered this answer to be exhaustive, and only during the last 10–15 year did I realize all the topicality of the question “What are you studying?” and the total inadequacy of my usual answer. This is related to the fact that in recent years the attention of both theorists and experimenters has focused on the question of the links of dynamics pertaining to averaged characteristics of problem solution to the solution behavior in specific realizations. This is especially relevant to geophysical problems related to the atmosphere and ocean in which, by and large, the respective averaging ensemble is absent and experimenters as a rule deal with individual realizations. In this case, the results of statistical analysis frequently not only have nothing in

common with the behavior of solutions in specific realizations but often simply contradict them. It is namely this that I would like to demonstrate in this report.

Three approaches are currently utilized in the analysis of a stochastic dynamical system.

The first approach is based on analyzing the Lyapunov stability of solutions to deterministic linear ordinary differential equations

$$\frac{d}{dt} \mathbf{x}(t) = A(t) \mathbf{x}(t)$$

and traditionally attracts the attention of many researchers. One analyzes here the upper bound of the problem solution

$$\lambda_{\mathbf{x}(t)} = \overline{\lim}_{t \rightarrow +\infty} \frac{1}{t} \ln |\mathbf{x}(t)|,$$

which is termed its characteristic exponent. When this approach is applied to stochastic dynamical systems, it is common that, to interpret and simplify the obtained results at the final stage, statistical analysis is invoked and statistical averages such, for example, as

$$\langle \lambda_{\mathbf{x}(t)} \rangle = \overline{\lim}_{t \rightarrow +\infty} \frac{1}{t} \langle \ln |\mathbf{x}(t)| \rangle,$$

are computed.

The drawbacks of this approach to stochastic dynamical systems are as follows:

(1) Such simplifying features of random parameters as stationarity in time, homogeneity, and isotropy in space are exploited only at the stage of final analysis.

(2) When passing to continual generalizations of ordinary differential equations (for example, in mechanics or the electrodynamics of continuous media), i.e., to partial differential equations (to fields), the analysis of Lyapunov stability is only possible through the series expansions of solutions in complete sets of orthogonal functions. If such a technique is applied to stochastic problems, a question emerges as to whether the operations of series expansion and statistical averaging are permutable. In particular, when statistical characteristics of random processes and fields are approximated by singular (generalized) functions (as, for example, in the approximation that fluctuations of system parameters are delta-correlated), these operations are not, as a rule, permutable.

The second approach is also traditional and relies on the analysis of moment and correlation functions of solutions to stochastic problems.

The drawback of this second approach is that commonly used methods of statistical averaging smooth the qualitative features of separate realizations and it is not uncommon for the obtained statistical characteristics to have nothing in common with the behavior of separate realizations.

In certain circumstances there exist, however, physical processes and phenomena occurring with the probability of one (i.e., happening in almost all realizations). They are called *coherent* (see monographs [1–4] and work [5] where this question is thoroughly discussed). To describe such phenomena, the third approach is applied. It is rooted in *the method of statistical topography* which studies, instead of moment functions, the statistical characteristics of some functionals describing precisely these coherent phenomena.

Below, we will illustrate these approaches as applied to simple physical problems.

2. Examples of dynamical systems

2.1 Diffusion of a passive inertialess admixture in a random velocity field

As the first example let us consider the relative diffusion of inertia-less particles in a random hydrodynamical flow with the velocity field $\mathbf{u}(\mathbf{r}, t)$ in the framework of the simplest kinematic equation for each particle:

$$\frac{d}{dt} \mathbf{r}(t) = \mathbf{u}(\mathbf{r}(t), t), \quad \mathbf{r}(0) = \mathbf{r}_0.$$

Numerical modeling of this problem indicates that the dynamics of the system of particles are essentially dependent on whether the velocity field is solenoidal or divergent. Thus, Fig. 1a presents in a schematic way a fragment of the evolution exhibited by a system of particles (a two-dimensional case) for a particular realization of a solenoidal velocity field $\mathbf{u}(\mathbf{r})$ stationary in time. Nondimensional time here is related to statistical parameters of the field $\mathbf{u}(\mathbf{r})$. Initially, the particles were uniformly spread over the circle. In this case, they continue to fill the area confined by the deformed contour in a fairly uniform way. Only a strong contour irregularity of a fractal character develops.

For the potential velocity field $\mathbf{u}(\mathbf{r})$, however, particles uniformly spread over a square at the initial instant of time form cluster areas as they evolve with time. Figure 1b presents a fragment of such an evolution, obtained through numerical simulation. We emphasize once again that formation of *clusters* in this case is a purely kinematic effect. Apparently, after averaging over an ensemble of realizations of the random velocity field this feature of the dynamics of particles will disappear.

Consider the joint dynamics of two particles. In this case, the probability density for the distance between the particles (provided the initial distance between them is small) is log-normal and moment functions of the distance (for example, in the two-dimensional case) grow with time exponentially:

$$\langle l^n(t) \rangle = l_0 \exp \left\{ \frac{1}{8} [2(D^s - D^p)n + 3D^p n^2] \right\},$$

where D^s and D^p pertain to the solenoidal and potential components of the spectral function of field $\mathbf{u}(\mathbf{r}, t)$.

There also exists a deterministic function called *the curve of typical realization* (CTR), which describes the main tendency of temporal behavior exhibited by the random process $l(t)$. For the problem considered here, this function, similarly, turns out to be an exponential function of time:

$$l^*(t) = l_0 \exp \left\{ \frac{1}{4} (D^s - D^p) t \right\},$$

and it is related to *the Lyapunov exponent*.

The CTR is essentially dependent on the sign of the difference $D^s - D^p$. In particular, for a solenoidal velocity field ($D^p = 0$) we have an exponentially growing typical realization. In the other limit, for a potential velocity field ($D^s = 0$), the typical realization is an exponentially decaying curve, i.e., particles would tend to coalesce. Consequently, *clusters* should form, i.e., zones of particle centering located in regions largely devoid of particles, which agrees with the results of numerical simulations. Thus, the inequality $D^s < D^p$ should hold for particle clustering in this problem.

The exponential growth of moments arises from overshoots of the process $l(t)$ relative to the curve of typical realization $l^*(t)$ both toward large and small values of l . It is a purely statistical effect caused by averaging over the entire ensemble of realizations.

Thus, we arrive at an apparent contradiction between the character of behavior exhibited by statistical characteristics of the process $l(t)$ and its behavior in concrete realizations. Let us formulate two clarifying remarks.

Remark 1. *The curve of typical realization (CTR)*

The statistical characteristics of a random process $z(t)$ are described by the probability density $P(t; z) = \langle \delta(z(t) - z) \rangle$ and integral distribution function

$$\begin{aligned} F(t; z) &= \text{Prob}(z(t) < z) = \langle \theta(z(t) - z) \rangle \\ &= \int_{-\infty}^z dz' P(t; z'), \end{aligned}$$

where $\delta(z)$ is the Dirac delta function, and $\theta(z)$ is the Heaviside function equal to 1 for $z > 0$, and to 0 for $z < 0$.

The curve of typical realization for the random process $z(t)$ is referred to as a deterministic curve $z^*(t)$ which is *the*

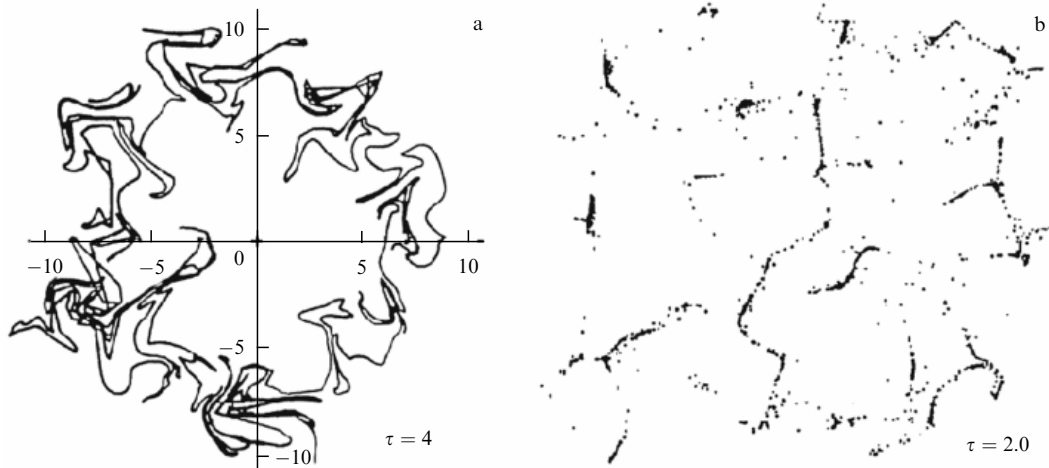


Figure 1. Results of modeling diffusion of a system of particles in solenoidal (a) and potential (b) random velocity fields.

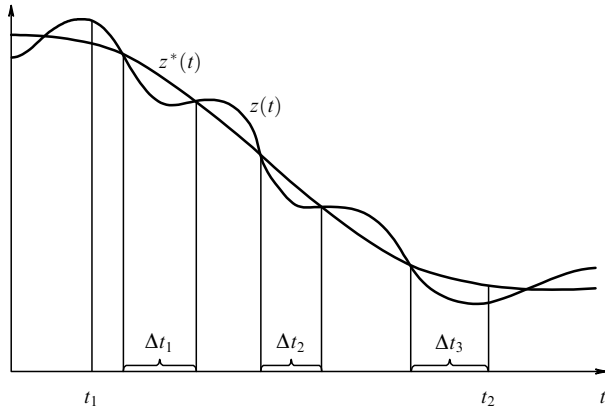


Figure 2. On the definition of the curve of typical realization for a random process.

median of the integral distribution function and is defined as a solution of the algebraic equation

$$F(t; z^*(t)) = \frac{1}{2}.$$

The motivation behind it is the property of a median that for any time interval (t_1, t_2) the random process $z(t)$ evolves as if it twists around the curve $z^*(t)$ in such a way that the mean time during which the inequality $z(t) > z^*(t)$ holds, coincides with the mean time during which the opposite inequality, $z(t) < z^*(t)$, is observed (Fig. 2), namely

$$\langle T_{z(t) > z^*(t)} \rangle = \langle T_{z(t) < z^*(t)} \rangle = \frac{1}{2} (t_2 - t_1).$$

The curve of typical realization, although obtained with the help of contemporaneous probability density, is defined, nevertheless, for any time $t \in (0, \infty)$.

For a Gaussian random process $z(t)$, the CTR coincides with the mean value of the process, namely $z^*(t) = \langle z(t) \rangle$.

Remark 2. Log-normal random process

Define the log-normal random process by means of a stochastic equation

$$\frac{d}{dt} y(t; \alpha) = [-\alpha + z(t)] y(t; \alpha), \quad y(0; \alpha) = 1,$$

where $z(t)$ is the Gaussian process with parameters $\langle z(t) \rangle = 0$ and $\langle z(t) z(t') \rangle = 2D\delta(t - t')$. Its contemporaneous probability density is described by the Fokker–Planck equation

$$\left(\frac{\partial}{\partial t} - \alpha \frac{\partial}{\partial y} \right) P(t; y, \alpha) = D \frac{\partial}{\partial y} y \frac{\partial}{\partial y} y P(t; y, \alpha),$$

$$P(0; y, \alpha) = \delta(y - 1).$$

The characteristic feature of the solution to this equation is the emergence of a long flattened tail for $Dt \gg 1$ implying the increased role of large overshoots of process $y(t; \alpha)$ in forming contemporaneous statistics. As a consequence of this, its moment functions

$$\langle y^n(t; \alpha) \rangle = \exp \left[n \left(n - \frac{\alpha}{D} \right) Dt \right],$$

$$\left\langle \frac{1}{y^n(t; \alpha)} \right\rangle = \exp \left[n \left(n + \frac{\alpha}{D} \right) Dt \right], \quad n = 1, 2, \dots$$

grow exponentially with time for $n > \alpha/D$.

For a log-normal process one finds $\langle \ln y(t) \rangle = -\alpha t$ and, consequently, the parameter $-\alpha = (1/t) \langle \ln y(t) \rangle$ is the *Lya-punov characteristic exponent*, while the CTR of the process $y(t; \alpha)$ turns out to be a curve exponentially decaying with time:

$$y^*(t) = \exp(\langle \ln y(t) \rangle) = \exp(-\alpha t).$$

Consider now a continual generalization to the problem of the diffusion of an inertialess passive admixture. In this case, the admixture density field $\rho(\mathbf{r}, t)$ is described by the continuity equation

$$\left(\frac{\partial}{\partial t} + \frac{\partial}{\partial \mathbf{r}} \mathbf{u}(\mathbf{r}, t) \right) \rho(\mathbf{r}, t) = 0, \quad \rho(\mathbf{r}, 0) = \rho_0(\mathbf{r}). \quad (1)$$

The total admixture mass is preserved as the admixture evolves with time, namely

$$M = M(t) = \int d\mathbf{r} \rho(\mathbf{r}, t) = \int d\mathbf{r} \rho_0(\mathbf{r}) = \text{const}.$$

To describe the local behavior of admixture field realizations in space in a random velocity field $\mathbf{u}(\mathbf{r}, t)$, one needs the probability distribution for the admixture density. Based on stochastic equation (1), we derive an equation for the probability density of the admixture density (concentration) field:

$$\left(\frac{\partial}{\partial t} - D_0 \Delta \right) P(\mathbf{r}, t; \rho) = D_\rho \frac{\partial^2}{\partial \rho^2} \rho^2 P(\mathbf{r}, t; \rho),$$

where the diffusion coefficient in the ρ -space, $D_\rho = D^\rho$, is only related to the potential component of field $\mathbf{u}(\mathbf{r}, t)$. The solution to this equation takes the form

$$P(\mathbf{r}, t; \rho) = \frac{1}{2\rho\sqrt{\pi Dt}} \exp \left(D_0 t \frac{\partial^2}{\partial \mathbf{r}^2} \right) \times \exp \frac{\ln^2 [\rho \exp(\alpha t) / \rho_0(\mathbf{r})]}{4Dt}. \quad (2)$$

If the initial admixture density is everywhere uniform, $\rho_0(\mathbf{r}) = \rho_0 = \text{const}$, the probability distribution of density is independent of \mathbf{r} and can be described by the equation

$$\frac{\partial}{\partial t} P(t; \rho) = D_\rho \frac{\partial^2}{\partial \rho^2} \rho^2 P(t; \rho). \quad (3)$$

From equation (3) it follows, in particular, that the probability distribution is log-normal and moment functions of the density field, beginning from the second one, exponentially grow with time $\tau = D_\rho t$:

$$\langle \rho^n(\mathbf{r}, t) \rangle = \rho_0^n \exp [n(n-1)\tau].$$

From the viewpoint of single-point characteristics of density field $\rho(\mathbf{r}, t)$, the problem in this case is statistically equivalent to a random process $\rho(t)$, whose probability density obeys Fokker–Planck equation (3), whereas the CTR exponentially decays with time at any fixed point in space:

$$\rho^*(t) = \rho_0 \exp(-\tau).$$

This gives evidence of the presence of a clustering behavior for fluctuations of medium density in arbitrary divergent flows.

The probability distribution (2) also enables learning about some characteristic features of the spatio-temporal structure of the density field realizations.

Remark 3. *Statistical topography of a random density field*

To be more illustrative, we limit ourselves here to the case of two dimensions as well. In statistical topography, important knowledge of the spatial behavior of realizations is provided by the analysis of isolines defined as

$$\rho(\mathbf{r}, t) = \rho = \text{const.}$$

In particular, the mean values of such functionals of the density field as the total area where $\rho(\mathbf{r}, t) > \rho$:

$$S(t, \rho) = \int d\mathbf{r} \theta(\rho(\mathbf{r}, t) - \rho) = \int d\mathbf{r} \int_{\rho}^{\infty} d\tilde{\rho} \delta(\rho(\mathbf{r}, t) - \tilde{\rho}),$$

and the total mass of the admixture comprised within this area:

$$\begin{aligned} M(t, \rho) &= \int d\mathbf{r} \rho(\mathbf{r}, t) \theta(\rho(\mathbf{r}, t) - \rho) \\ &= \int d\mathbf{r} \int_{\rho}^{\infty} d\tilde{\rho} \tilde{\rho} \delta(\rho(\mathbf{r}, t) - \tilde{\rho}), \end{aligned}$$

are defined by a single-point probability density and are expressed as

$$\begin{aligned} \langle S(t, \rho) \rangle &= \int_{\rho}^{\infty} d\tilde{\rho} \int d\mathbf{r} P(\mathbf{r}, t; \tilde{\rho}), \\ \langle M(t, \rho) \rangle &= \int_{\rho}^{\infty} d\tilde{\rho} \tilde{\rho} \int d\mathbf{r} P(\mathbf{r}, t; \tilde{\rho}). \end{aligned}$$

Hence, it is seen, in particular, that for $\tau \gg 1$ the mean area of the regions, where the density is in excess of a given level ρ , decays with time according to the law

$$\langle S(t, \rho) \rangle \approx \frac{1}{\sqrt{\pi\rho\tau}} \exp\left(-\frac{\tau}{4}\right) \int d\mathbf{r} \sqrt{\rho_0(\mathbf{r})},$$

while the mean mass of the admixture inside them, namely

$$\langle M(t, \rho) \rangle \approx M - \sqrt{\frac{\rho}{\pi\tau}} \exp\left(-\frac{\tau}{4}\right) \int d\mathbf{r} \sqrt{\rho_0(\mathbf{r})}$$

tends monotonically to the total mass. This once again confirms the conclusion drawn earlier that admixture particles tend to coalesce with time in clusters—the compact regions of augmented density surrounded by rarefied regions.

It should be noted that for a spatially homogeneous field $\rho(\mathbf{r}, t)$ these expressions can be simplified, yielding for specific quantities per unit area the following expressions

$$\langle s(t, \rho) \rangle = \int_{\rho}^{\infty} d\tilde{\rho} P(t; \tilde{\rho}), \quad \langle m(t, \rho) \rangle = \int_{\rho}^{\infty} d\tilde{\rho} \tilde{\rho} P(t; \tilde{\rho})$$

linked with the solution to equation (3).

2.2 Waves in a randomly inhomogeneous medium

As the second example, let us consider the problem of wave propagation in random media.

We begin with a one-dimensional problem which corresponds to waves in layered media.

Let a layer of a chaotically inhomogeneous medium occupy the space $L_0 < x < L$, and a plane wave $u_0(x) = \exp[-ik(x - L)]$ be incident on it from the region $x > L$. Due to the presence of inhomogeneities, there appears a wave reflected from the layer with the reflection coefficient $R_L = u(L) - 1$, and a wave leaving the layer with the transmission coefficient $T_L = u(L_0)$. Inside the layer, the wave field satisfies the boundary value problem:

$$\begin{aligned} \frac{d^2}{dx^2} u(x) + k^2[1 + \varepsilon(x)]u(x) &= 0, \\ u(L) + \frac{i}{k} \frac{du(x)}{dx} \Big|_{x=L} &= 2, \quad u(L_0) - \frac{i}{k} \frac{du(x)}{dx} \Big|_{x=L_0} = 0, \end{aligned}$$

where the function $\varepsilon(x)$, which we regard as a random one, describes the inhomogeneities of the medium.

Under the assumption that the statistical characteristics of function $\varepsilon(x)$ are known, the statistical problem amounts to searching for the statistical characteristics of the wave field intensity $I(x) = |u(x)|^2$ inside the inhomogeneous medium and at its boundaries.

A statistical analysis of the solution to this problem indicates that for a sufficiently thick layer, namely, $D(L - L_0) \gg 1$ [where the quantity D is related to statistical characteristics of $\varepsilon(x)$], $|T_L| \rightarrow 0$ with probability one and, consequently, $|R_L| \rightarrow 1$, i.e., the half-space ($L_0 \rightarrow -\infty$) of the randomly inhomogeneous medium totally reflects the incident wave. Thus, a *dynamical localization of the wave field* in this layer occurs.

However, the mean value of wave field intensity is constant in the half-space of the random medium, while higher moments normalized to their values at the layer boundary are described by the expression

$$\langle I^n(L - x) \rangle = \exp[Dn(n - 1)(L - x)],$$

i.e., the intensity of the wave field has a log-normal probability distribution, and moment functions grow exponentially along the direction deep into the medium.

In this case, the CTR for the wave intensity in the medium is described by an exponentially decaying function

$$I^*(x) = 2 \exp[-D(L - x)]$$

and coincides with the Lyapunov exponent; the quantity $l_{\text{loc}} = 1/D$, dubbed the *localization length*, sets the spatial scale for the decay of the wave field intensity in separate realizations.

Thus, it becomes apparent that the statistics form through large overshoots relative to the typical realization curve. Figure 3 shows two realizations of wave field intensity in a sufficiently thick layer, obtained through numerical simulations. It apparently illustrates the tendency of fast exponential decay (with large overshoots toward both ever larger intensity and zero).

Consider now wave propagation in a randomly inhomogeneous three-dimensional medium based on the scalar parabolic equation

$$\begin{aligned} \frac{\partial}{\partial x} U(x, \mathbf{R}) &= \frac{i}{2k} \Delta_{\mathbf{R}} U(x, \mathbf{R}) + \frac{ik}{2} \varepsilon(x, \mathbf{R}) U(x, \mathbf{R}), \\ U(0, \mathbf{R}) &= U_0(\mathbf{R}). \end{aligned} \quad (4)$$

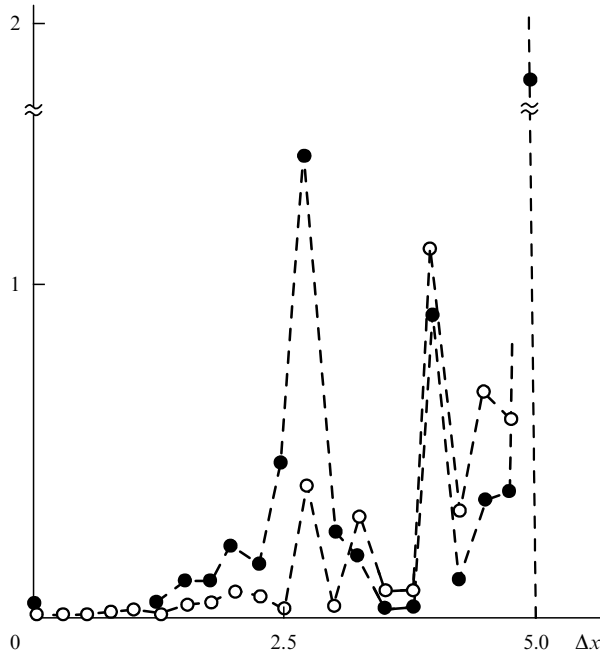


Figure 3. Numerical simulation of dynamic localization for two realizations of medium inhomogeneity.

Here, x is the coordinate in the direction of wave propagation, \mathbf{R} are the coordinates in the transverse plane, and $\varepsilon(x, \mathbf{R})$ is the deviation of permittivity from unity.

On introducing the amplitude and phase of the wave field as

$$U(x, \mathbf{R}) = A(x, \mathbf{R}) \exp \{iS(x, \mathbf{R})\},$$

the transfer equation can be written for the intensity of the wave field $I(x, \mathbf{R}) = |U(x, \mathbf{R})|^2$ in the form

$$\frac{\partial}{\partial x} I(x, \mathbf{R}) + \frac{1}{k} \nabla_{\mathbf{R}} \{ \nabla_{\mathbf{R}} S(x, \mathbf{R}) I(x, \mathbf{R}) \} = 0,$$

$$I(0, \mathbf{R}) = I_0(\mathbf{R}). \quad (5)$$

Hence, it follows that in the general case of an arbitrary incident beam the wave power in the plane $x = \text{const}$ is preserved:

$$E_0 = \int I(x, \mathbf{R}) d\mathbf{R} = \int I_0(\mathbf{R}) d\mathbf{R}.$$

Equation (5) shares its form with Eqn (1). It therefore can be treated as the transfer equation for a conservative admixture in a potential velocity field. As a consequence, realizations of the intensity field have a cluster character, whereas this clustering manifests itself through *caustic structures*. By way of example, Fig. 4 displays photos of a cross section of a laser beam propagating in a turbulent medium in a laboratory setup, for various fluctuations of permittivity. The appearance of the caustic structure of the wave field is vividly seen.

Let us introduce the amplitude and phase of the wave field and the complex phase of the wave:

$$U(x, \mathbf{R}) = A(x, \mathbf{R}) \exp (iS(x, \mathbf{R})) = \exp (\phi(x, \mathbf{R})),$$

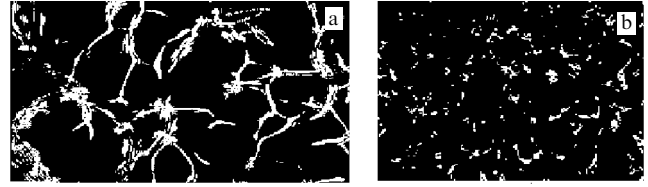


Figure 4. Cross section of a laser beam propagating in a turbulent medium in laboratory conditions (a) in the region of strong focusing, and (b) in the region of strong (saturated) fluctuations.

where

$$\phi(x, \mathbf{R}) = \chi(x, \mathbf{R}) + iS(x, \mathbf{R}).$$

$\chi(x, \mathbf{R}) = \ln A(x, \mathbf{R})$ is the wave amplitude level, and $S(x, \mathbf{R})$ is the wave phase fluctuations relative to the phase kx of the incident wave. Proceeding from parabolic equation (4), one can obtain, for the complex phase, a nonlinear equation of the so-called *Rytov method of smooth perturbations* (MSP):

$$\begin{aligned} \frac{\partial}{\partial x} \phi(x, \mathbf{R}) &= \frac{i}{2k} \Delta_{\mathbf{R}} \phi(x, \mathbf{R}) \\ &+ \frac{i}{2k} [\nabla_{\mathbf{R}} \phi(x, \mathbf{R})]^2 + i \frac{k}{2} \varepsilon(x, \mathbf{R}). \end{aligned}$$

For the case of a plane incident wave, which will only be considered further, it can be assumed that $U_0(\mathbf{R}) = 1$ without loss of generality and, consequently, that $\phi(0, \mathbf{R}) = 0$. In this case, the random field $\phi(x, \mathbf{R})$ is statistically homogeneous in the plane \mathbf{R} and all its single-point statistical characteristics are independent of the parameter \mathbf{R} .

Remark 4. *The Rytov smooth perturbation method*

The method of smooth perturbations was proposed by S M Rytov when analyzing the problem of light diffraction by ultrasonic waves in 1938. A M Obukhov applied this method in 1953 to treat the diffraction effects accompanying wave propagation in random media in the framework of perturbation theory. Earlier, analogous studies were carried out in the approximation of geometrical optics (acoustics). This technique has not lost its relevance even now providing the basic mathematical apparatus for various technical applications.

In the first order of the MSP, the statistical properties of amplitude fluctuations are characterized by the variance of amplitude level, i.e., by the parameter $\sigma_0^2(x) = \langle \chi_0^2(x, \mathbf{R}) \rangle$, in which case $\langle \chi_0(x, \mathbf{R}) \rangle = -\sigma_0^2(x)$. Regarding the variance of wave intensity, which is called the *scintillation index*, it is written down in the first approximation as

$$\begin{aligned} \beta_0(x) &= \langle I^2(x, \mathbf{R}) \rangle - 1 \\ &= \langle \exp [4\chi_0(x, \mathbf{R})] \rangle - 1 \approx 4\sigma_0^2(x). \end{aligned}$$

In this case, the intensity of the wave field is a log-normal random field and all statistical moments of the wave field intensity grow with an increase in the parameter $\beta_0(x)$, i.e., with the distance travelled by the wave. Now, a statistically equivalent random process $I(x)$ can be considered, for which the CTR of wave field intensity decays exponentially with distance:

$$I^*(x) = \exp \left(-\frac{1}{2} \beta_0(x) \right),$$

at any fixed point \mathbf{R} in space. This is indicative of the emergence of a cluster (caustic) structure in the intensity field. The formation of statistics (for instance, of moment functions $\langle I^n(x, \mathbf{R}) \rangle$) proceeds through large overshoots of the process $I(x)$ with respect to this curve.

The description of intensity fluctuations, obtained in the first order of the MSP, is valid for $\beta_0(x) \leq 1$. As the parameter $\beta_0(x)$ increases further, this approximation becomes violated and the nonlinear character of the equation for the complex phase of the wave field has to be taken into account. This range of fluctuations, called *the region of strong focusing*, is very difficult for analytical research. For even larger values of parameter $\beta_0(x)$, the statistical characteristics of intensity reach saturation, in which case $\beta(x) \rightarrow 1$ as $\beta_0(x) \rightarrow \infty$. This region of the parameter $\beta_0(x)$ variations is called *the region of strong intensity fluctuations*.

In this region, the statistical characteristics of the wave field cease to depend on the distance and one has

$$\langle I^n(x, \mathbf{R}) \rangle = n!, \quad P(x, I) = \exp(-I).$$

In this case, the mean specific area of regions within which $I(x, \mathbf{R}) > I$ and the mean specific power concentrated in these regions are constant and do not describe the behavior of the wave field intensity in separate realizations. Likewise, passage to a statistically equivalent random process is not informative in this case since its curve of typical realization assumes a constant value. An understanding of the wave field structure in specific realizations can only be gained in this case from the analysis of such quantities as the specific mean length of contours and mean specific number of wave field intensity contours. These quantities continue to grow with the parameter $\beta_0(x)$, implying that the splitting of contours takes place (see Fig. 4).

3. Conclusions

In closing, I would like to reiterate once more the main point of this talk. The approach to analysis of stochastic dynamical problems rooted in the ideas of stochastic topography, which enables, given the one-point statistical characteristics of processes and fields, determining quantitative and qualitative characteristics of behavior of their particular realizations for all times (in the entire space), has emerged as a result of discussions with experimenters who largely deal with separate realizations. For a comprehensive description of stochastic dynamical systems, it is insufficient to formulate a basic equations with respective boundary and initial conditions. It is necessary first and foremost to understand which coherent phenomena (occurring with the probability of unity, i.e., in almost all realizations of their solutions) are contained in these systems, and proceed with a statistical analysis in a related way.

The work was carried out with support from the Russian Foundation for Basic Research (projects Nos 07-05-006a and 07-05-92210-NtsNIL.a).

References

1. Klyatskin V I *Stokhasticheskie Uravneniya Glazami Fizika: Osnovnye Polozheniya, Tochnye Rezul'taty i Asimptoticheskie Priblizheniya* (Stochastic Equations through the Eye of the Physicist: Basic Concepts, Exact Results and Asymptotic Approximations) (Moscow: Fizmatlit, 2001) [Translated into English (Amsterdam: Elsevier, 2005)]

2. Klyatskin V I *Dinamika Stokhasticheskikh Sistem* (Dynamics of Stochastic Systems) (Moscow: Fizmatlit, 2002) [Translated into English (Amsterdam: Elsevier, 2005)]
3. Klyatskin V I *Diffuziya i Klasterizatsiya Passivnoi Primesi v Sluchainykh Gidrodinamicheskikh Potokakh* (Diffusion and Clusterization of Passive Tracers in Random Hydrodynamical Flows) (Moscow: Fizmatlit, 2005)
4. Klyatskin V I *Stokhasticheskie Uravneniya: Teoriya i Ee Prilozheniya k Akustike, Gidrodinamike i Radiofizike* (Stochastic Equations: Theory and its Applications to Acoustics, Hydrodynamics and Radiophysics) Vols 1, 2 (Moscow: Fizmatlit, 2008)
5. Klyatskin V I *Usp. Fiz. Nauk* **178** 419 (2008) [*Phys. Usp.* **51** 395 (2008)]

PACS numbers: 42.25.Dd, 42.68.Ay, 42.68.Xy
DOI: 10.3367/UFNe.0179.200905k.0553

Development of the radiative transfer theory as applied to instrumental imaging in turbid media

L S Dolin

1. Introduction

This talk presents the basic elements of instrumental imaging theory in media with strongly anisotropic scattering and a technique devised to compute images of diffusively reflecting objects, accounting for the effects of light absorption and multiple scattering. It discusses peculiarities of different variants of the radiative transfer equation in the small-angle approximation, used in the imaging theory and optical coherence ‘tomography’ (OCT) of turbid media. A new method of computing the temporal moments of a pulsed light beam transmitted through a layer of a turbid medium is described. The results of theoretical and experimental studies of shadow noises in OCT images of turbid media with fluctuating optical parameters are outlined.

By scattering light a turbid medium limits the visibility range of objects located within it and becomes visible itself. Therefore, the development of the methods and theory of instrumental imaging in turbid media was directed toward solving two interconnected tasks—the removal of the adverse influence of the medium on the visibility of objects, and the remote sensing of inherent optical properties of the medium itself.

The Koshmider equation [1] expresses the fundamental result of the imaging theory by relating the image contrast of a black object (observed in the sky background near the horizon) to the light attenuation coefficient in the atmosphere. The relationships for estimating the contrast of the image and visibility range of underwater objects under natural illumination were obtained in a now classical work by Duntley [2]. In this case, it was assumed that the angular size of the observed object is small, so that its apparent radiance is attenuated by the medium according to Buger's law. The need in a more universal imaging theory emerged in connection with the development of laser methods of underwater vision.

Pioneering works in this area were performed under the supervision of A V Gaponov-Grekhov in the Radiophysical Research Institute (NIRFI in *Russ. abbr.*) (Gor'ky) in the 1960s. They have led to the design of the first prototype of a laser-pulse system of underwater imaging with the help of

which the feasibility of an essential increase in the visibility range of underwater objects was demonstrated in sea conditions. It relied on laser target illumination and pulse gating of a useful signal. It was at that time that the main results laying the foundation for the modern theory of laser location and instrumental imaging in turbid media were obtained: based on the radiative transfer equation (RTE) in the small-angle approximation, an analytical model was proposed for blurring and attenuation of a laser beam in its passing through a medium with strongly anisotropic scattering [3, 4]; formulas were derived for gauging the characteristics of underwater object images taking into account the effects of light absorption and multiple scattering in water [5–10], and a universal technique was suggested for estimating the potential range of underwater imaging systems of different types, including laser-based ones [11–14].

The plausibility of applying the phenomenological radiative transfer theory to the analysis of coherent light beam propagation in a turbid medium was a subject of certain concern. It was partly removed owing to Refs [15–17], which derived the equation for the coherence function of a wave beam in a medium with strongly anisotropic scattering and showed that the Fourier transform of the coherence function satisfies the RTE in the small-angle approximation and, consequently, that it is a wave analogue to the light field radiance (these results were reported at S M Rytov's seminar in 1966, through the initiative of M A Miller who was in charge of theoretical research in hydrooptics at NIRFI and offered everyday help with his advice and criticism to researchers involved in this work). The justification of RTE in a more general formulation was a subject of intensive research, with results reported in a set of reviews and monographs [18–20].

Later on, different variants of RTE solutions in the small-angle approximation were used for developing the theory of laser location and imaging of underwater objects through a rough sea surface and lidar methods of determining the optical characteristics of natural scattering media, and also in problems concerning the optical tomography of biological tissues.

2. How to build a model image on the basis of the radiative transfer equation

When solving the problems of imaging theory in turbid media one can assume, without loss of generality, that the observing system (Fig. 1) comprises the illuminating source S and optical receiver R, whereas the image is formed by detecting the power of the incoming signal P_R as a function of coordinates \mathbf{r}_0 of the point at which the axes of the directivity patterns of the source \mathbf{n}_S and the receiver \mathbf{n}_R intersect the surface of the object S_{ob} . To determine the signal P_R , the radiative transfer equation [21] is applied:

$$\left(\frac{1}{c} \frac{\partial}{\partial t} + \mathbf{n} \nabla_{\mathbf{r}} + \alpha \right) I(\mathbf{r}, \mathbf{n}, t) = \sigma \int_{4\pi} I(\mathbf{r}, \mathbf{n}', t) x(\gamma) d\mathbf{n}' + Q, \quad (1)$$

where $I(\mathbf{r}, \mathbf{n}, t)$ is the intensity of radiation (radiance) at a point in space \mathbf{r} in the direction of unit vector \mathbf{n} at the instant of time t , c and $\alpha = \sigma + \kappa$ are the speed of light and attenuation coefficient in the medium, respectively, σ and κ are the scattering and absorption coefficients, $x(\gamma)$ is the scattering phase function normalized as $2\pi \int_0^\pi x(\gamma) \sin \gamma d\gamma = 1$,

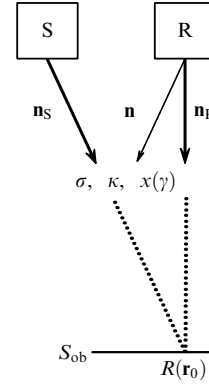


Figure 1. Schematics of observations.

$\gamma = \arccos(\mathbf{n}\mathbf{n}')$ is the scattering angle, $d\mathbf{n}'$ is the solid angle element around the direction \mathbf{n}' , and Q are the volume sources of radiation.

Scattering phase functions of natural turbid media exhibit well-expressed anisotropy. They therefore can be described with sufficient accuracy by the expression

$$x(\gamma) = (1 - 2p_b) x_1(\gamma) + \frac{p_b}{2\pi}, \quad (2)$$

where $p_b = 2\pi \int_{\pi/2}^\pi x(\gamma) \sin \gamma d\gamma$ is the backscattering probability, $p_b \ll 1$, $x_1(\gamma)$ is the narrow part of the scattering phase function satisfying the conditions $2\pi \int_0^\pi x_1(\gamma) \sin \gamma d\gamma = 1$, and $x_1(\gamma) \ll p_b/(2\pi)$ for $\gamma > \pi/2$. The power of a received signal $P_R(\mathbf{r}_0, t)$ is expressed through the radiance of light $I_R(-\mathbf{n}, t)$ incident on the receiver aperture as

$$P_R(\mathbf{r}_0, t) = \Sigma_R \int I_R(-\mathbf{n}, t) D_R(\vartheta) d\mathbf{n},$$

where Σ_R is the area of the detector entrance pupil, and $D_R(\vartheta)$ is its directivity pattern: $D_R(0) = 1$, $\vartheta = \arccos(\mathbf{n}\mathbf{n}_R)$. The light field from source S is expanded as a sum of 'directed' I_1 and diffusive I_2 components. The first of them plays the major role in illuminating the object, while the second one corresponds to a signal reflected by the medium (backscattering noise, 'haze'). The field I_1 is identified with that emitted by the source S in an 'auxiliary' medium with a narrow scattering phase function $x_1(\gamma)$, scattering coefficient $\sigma_1 = \sigma - 2\sigma_b$, and absorption coefficient $\kappa_1 = \alpha - \sigma_1 = \kappa + 2\sigma_b$, where $\sigma_b = p_b\sigma$ is the backscattering coefficient of the real medium. Computation of the diffusive field component in the approximation of single light scattering over large angles reduces to finding the field of distributed radiation sources

$$Q = \frac{\sigma_b}{2\pi} \int_{4\pi} I_1 d\mathbf{n}$$

in the auxiliary medium. In this case, the total power of the received signal is presented in the form

$$P_R = P_{ob} + P_b, \quad (3)$$

$$P_{ob} = \frac{\Sigma_R \Omega_R}{\pi} \iint_{S_{ob}} R(\mathbf{r}') \times \left[\int_{-\infty}^{\infty} E^{(s)}(\mathbf{r}', t') E^{(r)}(\mathbf{r}', t - t') dt' \right] d\mathbf{r}', \quad (4)$$

$$P_b = \frac{\Sigma_R \Omega_R}{2\pi} \iiint_V \sigma_b(\mathbf{r}) \times \left[\int_{-\infty}^{\infty} E_0^{(s)}(\mathbf{r}, t') E_0^{(r)}(\mathbf{r}, t - t') dt' \right] d\mathbf{r}, \quad (5)$$

where P_{ob} is the signal power from the object; P_b is the power of the volume backscattering signal; $\Omega_R = 2\pi \int_0^{\pi/2} D_R(\vartheta) \sin \vartheta d\vartheta$ is the effective solid receiving angle; $E^{(s)}(\mathbf{r}', t) = \int_{\mathbf{n} \cdot \mathbf{N} > 0} (\mathbf{n} \cdot \mathbf{N}) I_1 d\mathbf{n}$ and $E_0^{(s)}(\mathbf{r}, t) = \int_{4\pi} I_1 d\mathbf{n}$ are the irradiance of the object surface at point \mathbf{r}' and spatial irradiation of the medium at point \mathbf{r} at the instant of time t , and $E^{(r)}(\mathbf{r}', t)$ and $E_0^{(r)}(\mathbf{r}, t)$ are, respectively, the irradiance of the object and medium due to an auxiliary δ -pulse source of light with a unit energy and the directivity pattern of the detector. The integration in formula (4) is performed over the object's surface S_{ob} , whereas that in formula (5) is carried out over the illuminated volume V of the medium. For a stationary illumination (when functions with superscript (s) are time independent), the time convolution drops out from formulas (4) and (5), and the functions with superscript (r) in the integrands become irradiances of the object and medium from the auxiliary continuous light source with unit power. Formulas (3)–(5) allow the received signal to be expressed through the reflection coefficient of the observed object, backscattering coefficient of the turbid medium, and irradiation fields created by the real and auxiliary radiation sources in a turbid medium that scatters light only 'forward'.

For the given positions of the source, the detector, and the object of observation, the functions $E^{(s,r)}$ and $E_0^{(s,r)}$ in Eqns (4) and (5) depend not only on variables \mathbf{r} , \mathbf{r}' and t , but also on the coordinates of object point \mathbf{r}_0 , toward which point the directivity patterns of the source and detector. If the field of view of the observing system is sufficiently small and the distance z_{ob} to the object is large compared to the 'source–detector' base, then, for stationary object illumination, the dependence of the signal P_{ob} on \mathbf{r}_0 is given by the formulas

$$P_{ob}(\mathbf{r}_0, z_{ob}) = \frac{P_S}{\pi} \iint_{S_{ob}} R(\mathbf{r}') A_{ob}(\mathbf{r}_0 - \mathbf{r}', z_{ob}) d\mathbf{r}', \quad (6)$$

$$A_{ob}(\mathbf{r}_\perp, z) = \Sigma_R \Omega_R \bar{E}^{(s)}(\mathbf{r}_\perp, z) \bar{E}^{(r)}(\mathbf{r}_\perp, z), \quad (7)$$

where P_S is the power of the illuminating source, and $\bar{E}^{(s,r)}$ is the distribution of irradiance in the plane $z = \text{const}$ due to real and auxiliary illuminating beams with unit power, when the beam axes are oriented toward a point $\mathbf{r}_\perp = 0$ in this plane.

The functions $\bar{E}^{(s,r)}$ could be termed the effective directivity patterns of the source and receiver. In order to retrieve the image, at least one of them should be narrow. In the standard television system, an image is formed owing to the directivity pattern $\bar{E}^{(r)}$, and in a system with a running light beam, owing to $\bar{E}^{(s)}$. According to Eqn (6), a turbid medium transforms the image as a linear filter of two-dimensional signals. The function $A_{ob}(\mathbf{r}_\perp, z)$, dubbed the point spread function (PSF), characterizes the structure of the image of a pointwise object and serves as an analogue of the pulse characteristic for filters of electric signals. To find this function, it suffices to know the directivity patterns of the source and detector and the distribution of irradiance $e(r_\perp, z)$ in a cross section of an infinitely narrow light beam transmitted through a medium layer of thickness z . The normalized spatial spectrum of

this distribution,

$$T(k, z) = \frac{\int_0^\infty e(r_\perp, z) J_0(kr_\perp) r_\perp dr_\perp}{\int_0^\infty e(r_\perp, z) r_\perp dr_\perp},$$

is called the modulation transfer function of the turbid medium layer.

For a pulse illumination of the object, the energy of a useful signal at the image element can be estimated from Eqns (6) and (7): $W_{ob}(\mathbf{r}_0) = \int P_{ob}(\mathbf{r}_0, t) dt$. This knowledge is what is needed to estimate the image quality. When computing W_{ob} it is necessary to make the substitutions in Eqn (6): $P_{ob} \rightarrow W_{ob}$ and $P_S \rightarrow W_S$, where W_S is the energy of the sounding pulse.

If a turbid medium is sounded with light pulses of duration Δt , a signal backscattered at an instant t returns from the depth $z_t = ct/2$ from a layer with a thickness of $c\Delta t/2$. As follows from Eqn (5), if the optical axes of the source and detector are directed toward the point \mathbf{r}_0 in the plane $z = z_t$, the power of the detected signal is expressed in the form

$$P_b(\mathbf{r}_0, z_t) = \frac{cW_S}{4\pi} \iint_{\infty} \sigma_b(\mathbf{r}_\perp, z_t) A_b(\mathbf{r}_0 - \mathbf{r}_\perp, z_t) d\mathbf{r}_\perp, \quad (8)$$

$$A_b(\mathbf{r}_\perp, z) = \Sigma_R \Omega_R \bar{E}_0^{(s)}(\mathbf{r}_\perp, z) \bar{E}_0^{(r)}(\mathbf{r}_\perp, z) \quad (9)$$

through the medium backscattering coefficient σ_b and distributions $\bar{E}_0^{(s,r)}(\mathbf{r}_\perp, z)$ of spatial irradiance in the cross section of real and auxiliary light beams at a distance z from the source. Formulas (8) and (9) are applicable provided the pulse length $c\Delta t$ is small relative to the photon mean free path $1/\alpha$ and the scale Δz of longitudinal inhomogeneity σ_b . They indicate that the pulse imaging system is equally applicable to observing objects in a turbid medium and spatial variations of the backscattering coefficient of the medium proper. The distributions $\bar{E}_0^{(s,r)}$ and $\bar{E}^{(s,r)}$ differ only slightly in an auxiliary medium with a narrow scattering indicatrix. Thus, computing images of the object or medium, one can set $A_b(\mathbf{r}_\perp, z) \approx A_{ob}(\mathbf{r}_\perp, z)$ and use one and the same PSF.

Formulas (8) and (9) underlie the theory of laser sounding of the ocean and atmosphere and algorithms for the remote assessment of their optical characteristics. These formulas can also be adapted to describe images of a scattering medium, obtained using the method of optical coherence tomography [22]. In OCT setups, a continuous light is used with femtosecond coherence times and the interferometric method is exploited to determine the depth from which the backscattered signal comes. Optical signals are emitted and received by the end of a single-mode optical fiber. This creates conditions for the backscattering amplification effect to manifest itself [23], which is missing from the transfer equation. In order to address it, the development of a wave model of OCT-imaging [24] was needed, relying on the hybrid method of evaluating field fluctuations in a medium with coarse and fine inhomogeneities of permittivity [25]. It was shown [24] that the OCT system with a heterodyne detector can be brought into correspondence with an equivalent system of pulse location with direct signal detecting, while the specifics of the single-position sounding method can be taken into account by setting

$$A_b(\mathbf{r}_\perp, z) = \Sigma_R \Omega_R [2E^2(\mathbf{r}_\perp, z) - E_{ns}^2(\mathbf{r}_\perp, z)]$$

in Eqn (8), where E is the total irradiance of the medium at point \mathbf{r}_\perp, z , and E_{ns} is the medium irradiance through nonscattered (direct) light from the source.

Thus, the theory of stationary light beam propagation in a medium with a narrow scattering indicatrix can serve as a basis for computing images formed by active vision systems, both continuous and pulsed. In order to analyze the performance of passive observing facilities, one also needs a model of a natural light field.

3. Analytical models of light fields for problems of imaging theory

The theory describing the propagation of a narrow light beam in media with strongly anisotropic scattering relies on the radiative transfer equation in the small-angle approximation [12]. Assuming that the beam propagates in the direction of the z -axis, this equation can be cast in the form

$$\left[c^{-1} \frac{\partial}{\partial t} + n_z \frac{\partial}{\partial z} + \mathbf{n}_\perp \nabla_\perp + \alpha \right] I(\mathbf{r}_\perp, z, \mathbf{n}_\perp, t) = \sigma_1 \iint_{\infty} I(\mathbf{r}_\perp, z, \mathbf{n}'_\perp, t) x_1(|\mathbf{n}_\perp - \mathbf{n}'_\perp|) d\mathbf{n}'_\perp, \quad (10)$$

where \mathbf{r}_\perp and \mathbf{n}_\perp are the components of \mathbf{r} and \mathbf{n} in the plane $z = \text{const}$, and $n_z = (1 - n_\perp^2)^{1/2}$.

A rigorous analytical solution of Eqn (10) can only be obtained in the approximation $n_z \approx 1$, which ignores the effects of photon multipath propagation (distortion of the light signal as it travels through the medium, the formation of stationary angular radiance distribution in a continuous beam at large optical distances from its source). Originally, this equation was exploited in the theory of multiple scattering of fast charged particles in matter [26–29]; with its assistance, an expression for the angular distribution of particles in an infinitely broad beam was found [26, 27] and the functions of the type $\iint_{\infty} I(x, y, z, n_x, n_y) dy dn_y$, which characterize the structure of a thin beam, were analyzed [28]. The solution to Eqn (10) at $n_z = 1$ and an arbitrary boundary condition for the radiance at the source aperture, $I(\mathbf{r}_\perp, 0, \mathbf{n}_\perp) = I_0(\mathbf{r}_\perp, \mathbf{n}_\perp)$, was obtained in Ref. [3] and later generalized for stratified turbid media in Ref. [30]. According to this solution, the distribution of irradiance $E(\mathbf{r}_\perp, z) = \iint_{\infty} I d\mathbf{n}_\perp$ over the cross section of a light beam exiting the layer of a turbid medium with a narrow scattering phase function $x_1(\gamma)$ and optical parameters $\alpha(z)$, $\sigma_1(z)$, and $\kappa_1(z) = \alpha - \sigma_1$ is expressed in a spectral form as

$$E(\mathbf{r}_\perp, z) = \iint_{\infty} F(\mathbf{k}, z) T(k, z) \exp(-\tau_\kappa + i\mathbf{k}\mathbf{r}_\perp) d\mathbf{k} \quad (11)$$

through the functions

$$F = \frac{1}{(2\pi)^2} \iint_{\infty} \iint_{\infty} I_0(\mathbf{r}_\perp, \mathbf{n}_\perp) \exp[-i\mathbf{k}(\mathbf{r}_\perp + z\mathbf{n}_\perp)] d\mathbf{r}_\perp d\mathbf{n}_\perp, \\ T = \exp \left[- \int_0^z \sigma_1(z - z') [1 - x_S(kz')] dz' \right], \quad (12) \\ \tau_\kappa = \int_0^z \kappa_1(z') dz', \quad x_S(p) = 2\pi \int_0^\infty x_1(\gamma) J_0(p\gamma) \gamma d\gamma,$$

the first of which (F) determines the beam structure at a distance z from the source in an absolutely transparent medium, while the second (T) represents the modulation

transfer function of the turbid medium layer through which the beam was traveling.

Equation (10) served as a ‘bridge’ connecting for the first time the theory of radiative transfer with that of wave propagation in randomly inhomogeneous media. This link was made explicit when considering the propagation of a wave beam $u = V(\mathbf{r}_\perp, z) \exp(i\omega t - ikz)$ through a medium with the large-scale fluctuations of permittivity $\varepsilon = \langle \varepsilon \rangle [1 + \delta\varepsilon(\mathbf{r}_\perp, z)]$. Based on the equation

$$\left[\Delta_\perp - 2ik \frac{\partial}{\partial z} + k^2 \delta\varepsilon \right] V = 0$$

for the field correlation function

$$\Gamma(\mathbf{r}_\perp, z, \rho_\perp) = \left\langle V\left(\mathbf{r}_\perp + \frac{\rho_\perp}{2}, z\right) V^*\left(\mathbf{r}_\perp - \frac{\rho_\perp}{2}, z\right) \right\rangle, \quad (13)$$

an equation of the form [16, 17]

$$\left\{ \nabla_{\mathbf{r}_\perp} \nabla_{\rho_\perp} - ik \frac{\partial}{\partial z} - ik^2 [b(0) - b(\rho_\perp)] \right\} \Gamma = 0,$$

$$b(\rho_\perp) = \frac{k}{4} \int_{-\infty}^{\infty} \langle \delta\varepsilon(\mathbf{r}_\perp + \rho_\perp, z + \xi) \delta\varepsilon(\mathbf{r}_\perp, z) \rangle d\xi,$$

$$k = \omega \frac{\sqrt{\langle \varepsilon \rangle}}{c}$$

was derived. It was also shown that the Fourier transform of the correlation function:

$$I(\mathbf{r}_\perp, z, \mathbf{n}_\perp) = \frac{1}{\lambda^2} \iint_{\infty} \Gamma(\mathbf{r}_\perp, z, \rho_\perp) \exp(i\mathbf{k}\mathbf{n}_\perp \rho_\perp) d\rho_\perp, \\ \lambda = \frac{2\pi}{k}, \quad (14)$$

satisfies Eqn (10) with the coefficient $n_z = 1$, describing the radiation field in a medium with optical characteristics

$$x_1(n_\perp) = \frac{2\pi}{\lambda^2 b(0)} \int_0^\infty b(\rho_\perp) J_0(kn_\perp \rho_\perp) \rho_\perp d\rho_\perp,$$

$$\sigma_1 = kb(0), \quad \kappa_1 = 0.$$

The implication was that the mathematical apparatus of the radiative transfer theory can be employed to analyze the influence of a randomly inhomogeneous medium on the correlation and energy characteristics of a wave beam with due regard for its diffractive broadening, provided that its radiance is defined not in the energy terms (as the radiation flux per unit area and per unit solid angle), but through relationship (14).

The influence of a photon spread in ranges on the characteristics of nonstationary light fields was explored with the help of an equation of the Fokker–Planck type [12]:

$$\left[\frac{1}{c} \frac{\partial}{\partial t} + n_z \frac{\partial}{\partial z} + \mathbf{n}_\perp \nabla_\perp + \kappa_1 - \frac{d_2}{4} \sigma_1 \Delta_{\mathbf{n}_\perp} \right] I(\mathbf{r}_\perp, z, \mathbf{n}_\perp, t) = 0 \quad (15)$$

with the coefficient $n_z = 1 - n_\perp^2/2$. Equation (15) follows from Eqn (10) under the condition that the scattering phase function be narrow compared to the width of angular radiance distribution, and contain only the integral indicatrix parameter $d_2 = 2\pi \int_0^\pi \gamma^2 x_1(\gamma) \sin \gamma d\gamma$. On the basis of

Eqn (15), a theory of multiple scattering for sinusoidally modulated light beams was developed [31]. It was shown that the sinusoidal component of the radiation field behaves similarly to a wave with specific dispersive properties. This equation was exploited as well for the analysis of the spatio-temporal structure of a pulsed light beam [32] and the construction of simple analytical models of stationary radiation fields formed by sources of various types in strongly absorbing media with narrow scattering phase functions [33].

The radiation field of a δ -pulsed source $Q(\mathbf{r}, \mathbf{n}, t) = \bar{Q}(\mathbf{r}, \mathbf{n}) \delta(t)$ in a turbid medium with an absorption coefficient κ_1 is expressed in the form

$$I = \frac{1}{2\pi} \int \bar{I}(\mathbf{r}, \mathbf{n}, \kappa_1 + i \frac{\omega}{c}) \exp(i\omega t) d\omega$$

through the solution $\bar{I}(\mathbf{r}, \mathbf{n}, \kappa_1)$ of the transfer equation with a stationary source $\bar{Q}(\mathbf{r}, \mathbf{n})$. Hence, the integral parameters of the pulsed signal—its mean propagation time \bar{t} and typical duration Δt —can be found by differentiating $\bar{I}(\mathbf{r}, \mathbf{n}, \kappa_1)$ with respect to the parameter κ_1 :

$$\bar{t} = \frac{\int t I dt}{\int I dt} = -\frac{1}{c} \frac{d \ln \bar{I}}{d \kappa_1}, \quad (16)$$

$$(\Delta t)^2 = \frac{\int (t - \bar{t})^2 I dt}{\int I dt} = \frac{1}{c^2} \frac{d^2 \ln \bar{I}}{d \kappa_1^2}. \quad (17)$$

Owing to relationships (16) and (17), the models of stationary radiation fields presented above turn out to be very useful also for the theory of pulsed signal propagation in turbid media.

The spatial structure of a narrow light beam is described by Eqn (15) with a large error. For this reason, Eqn (10) with the coefficient $n_z = 1 - n_\perp^2/2$, which is devoid of this drawback, holds some interest for a certain set of applications. Based on this equation, a theory was developed for plane pulsed wave propagation in a turbulent medium [34]. An approximate solution to this equation was also obtained for a monodirectional δ -pulsed source [35]. The analysis of this solution has, in particular, shown that the time moment (17) is determined from Eqn (15) with a noticeable error and depends not only on the scattering phase function dispersion d_2 , but also on the parameter

$$g = \frac{2\pi}{d_2^2} \int_0^\pi \gamma^4 x_1(\gamma) \sin \gamma d\gamma,$$

which characterizes its form.

The absence of an exact analytical solution to Eqn (10) with the coefficient $n_z = 1 - n_\perp^2/2$ does not exclude the possibility of finding the integral characteristics of its exact solution. If one passes on in Eqn (10) to dimensionless variables [34] $s = ct$ and $\zeta = ct - z$, then for the moments of longitudinal radiance distribution in the pulse volume, viz.

$$M_m(\mathbf{r}_\perp, \mathbf{n}_\perp, s) = \int_0^\infty \zeta^m I(\mathbf{r}_\perp, \zeta, \mathbf{n}_\perp, s) d\zeta, \quad m = 0, 1, \dots, \quad (18)$$

follow the equations [36]

$$\begin{aligned} & \left(\frac{\partial}{\partial s} + \mathbf{n}_\perp \nabla_\perp + \alpha \right) M_m(\mathbf{r}_\perp, \mathbf{n}_\perp, s) \\ &= \sigma_1 \int_{-\infty}^\infty M_m(\mathbf{r}_\perp, \mathbf{n}'_\perp, s) x_1(|\mathbf{n}_\perp - \mathbf{n}'_\perp|) d\mathbf{n}'_\perp + \frac{m}{2} n_\perp^2 M_{m-1}, \end{aligned} \quad (19)$$

which yield the exact analytical solution because they are identical to the stationary equation (10) with the coefficient $n_z = 1$. The moment M_0 is found directly by replacing $z \rightarrow s$, $I \rightarrow M_0$, and $I_0 \rightarrow M_0(\mathbf{r}_\perp, \mathbf{n}_\perp, 0)$, while computation of the higher moments requires solving the RTE with volume sources. Notice that temporal moments of the radiation field can easily be expressed through the spatial ones (M_m), provided the shape of the light pulse varies only slightly as it displaces over the proper length.

4. Fluctuating light fields and images

Random distortions of images occur when objects are observed through a turbulent atmosphere, rough water surface, or turbid medium, the optical parameters of which vary randomly in space (when the Earth is observed from space, the role of such a medium can be played by fragmented cloudiness). In order to analyze the influence of turbulence on images, the wave theory is routinely used; in the other cases mentioned above, the methods and apparatus of the radiative transfer theory are employed.

The theory of instrumental imaging through the rough water surface [37, 38] is similar to that of underwater imaging in the sense that in both cases the signals from the object and the medium are determined from relationships (4) and (5). The influence of the surface on the image is taken into account by substituting fields $E^{(s,r)}$ found with regard for light refraction at the air–water interface into these relationships. The fields $E^{(s,r)}$ are expressed through the radiance of light incident on the water surface and Green's function of the transfer equation in the small-angle approximation. This yields the general expression for a random realization of an image, which is further used to analyze its statistical characteristics. One need not solve the transfer equation all over again.

The theory of imaging in turbid media with fluctuating optical characteristics calls for qualitatively new solutions to the RTE. Such solutions are also necessary for problems of the optical diagnostics of similar media. The research on light propagation in turbid media with randomly inhomogeneous optical characteristics was initially prompted by problems of Earth's radiative balance [39]. In that case, relatively simple models of scattering objects were employed (a homogeneous layer of turbid medium with a fluctuating optical thickness or a smoothly inhomogeneous layer). Later on, the focus shifted toward statistical models of radiative transfer in media with three-dimensional concentration inhomogeneities of absorbing and scattering substances [40–43]. Along with models of the statistically mean radiation field, the models of its fluctuations were developed, too. In particular, equations have been obtained for computing the mean radiance and the function of the spatial radiance correlation for a light beam leaving a layer of a turbid medium with a narrow scattering phase function and randomly inhomogeneous coefficients of absorption and scattering [41]. These equations have allowed one to quantitatively describe the bleaching effect of the medium, caused by fluctuations in its parameters, and also the processes of random modulation of radiance distribution in a narrow light beam upon its multiple passing through absorbing inhomogeneities and the 'smoothing' of occurring radiance fluctuations because of multiple 'forward' scattering. It was shown that relative radiance fluctuations can grow without limits as the thickness of the scattering layer increases and that a stationary regime of fluctuations (their saturation)

can settle down depending on the medium parameters [41, 44, 45].

These equations served as a basis for developing a statistical model of OCT — imaging of a layered turbid medium with three-dimensional inhomogeneities of absorption and backscattering coefficients $\kappa = \bar{\kappa}(z) + \tilde{\kappa}(\mathbf{r}_\perp, z)$ and $\sigma_b = \bar{\sigma}(z) + \tilde{\sigma}(\mathbf{r}_\perp, z)$, ($\bar{\kappa} = \langle \kappa \rangle$, $\bar{\sigma} = \langle \sigma_b \rangle$), respectively. Expressions for spatial correlation function $B_P(\mathbf{p}, z_1, z_2)$ of relative fluctuations of tomographic signal power $P(\mathbf{r}_\perp, z)$, coming from two separate locations within a medium with coordinates $\mathbf{r}_\perp + \mathbf{p}/2, z_1$ and $\mathbf{r}_\perp + \mathbf{p}/2, z_2$, were found and it was shown that fluctuations of medium parameters lead to the appearance of spatial noise with specific properties ('shadow' noise) [46, 47] in the medium image. This noise arises as a result of inhomogeneous shading of each medium layer by clusters of the absorbing or scattering substance located in the upper layers. Notice that fluctuations of κ are manifested only through the shadow noise, while those of σ_b show up through the shadow noise and images of inhomogeneities σ_b proper. Figures 2 and 3 give examples of function $B_P(\mathbf{p}, z_1, z_2)$ computed for those cases when only one of these parameters fluctuates. The computations used the formulas

$$B_P(\mathbf{p}, z_1, z_2) = \left\{ \left[1 - \frac{4A_\sigma(\mathbf{p}, z_m)}{\bar{\sigma}(z_m) - 2A_\sigma(0, z_m)} + \frac{B_\sigma(\mathbf{p}, z, \xi)}{[\bar{\sigma}(z_1) - 2A_\sigma(0, z_1)][\bar{\sigma}(z_2) - 2A_\sigma(0, z_2)]} \right] \times \exp \left[\int_0^{z_m} [4A_\kappa(\mathbf{p}, z') + 16A_\sigma(\mathbf{p}, z')] dz' \right] \right\} - 1, \quad (20)$$

$$A_\kappa(\mathbf{p}, z) = \int_{-\infty}^{\infty} B_\kappa(\mathbf{p}, z, \xi) d\xi, \quad (21)$$

$$A_\sigma(\mathbf{p}, z) = \int_{-\infty}^{\infty} B_\sigma(\mathbf{p}, z, \xi) d\xi,$$

$$B_\kappa(\mathbf{p}, z, \xi) = \left\langle \tilde{\kappa} \left(\mathbf{r} + \frac{\mathbf{p}}{2}, z + \frac{\xi}{2} \right) \tilde{\kappa} \left(\mathbf{r} - \frac{\mathbf{p}}{2}, z - \frac{\xi}{2} \right) \right\rangle, \quad (22)$$

$$B_\sigma(\mathbf{p}, z, \xi) = \left\langle \tilde{\sigma} \left(\mathbf{r} + \frac{\mathbf{p}}{2}, z + \frac{\xi}{2} \right) \tilde{\sigma} \left(\mathbf{r} - \frac{\mathbf{p}}{2}, z - \frac{\xi}{2} \right) \right\rangle, \quad (23)$$

$$z = \frac{z_1 + z_2}{2}, \quad \xi = z_1 - z_2, \quad z_m = z - \frac{1}{2} |\xi|, \quad (24)$$

which are applicable under the condition that the width of the PSF be small compared to the typical horizontal size of inhomogeneities. As follows from the figures, fluctuations of the absorption coefficient lead to the appearance of noise, the correlation function of which is everywhere positive and has the shape of a wave crest. When the backscattering coefficient is fluctuating, the correlation function can change its sign since the image of each inhomogeneity and its shadow form the combined signal with sign-changing intensity variations.

These theoretical conclusions got qualitative support from experiments with a model turbid medium containing absorbing inhomogeneities and the results of correlation processing of biotissue tomograms. Figure 4 presents a comparison between the theoretical and experimental dependences of dispersion in relative fluctuations of tomographic signal power $d_P(z) = B_P(0, z, z)$ on the depth z it originated from. In processing the tomograms, the following functions

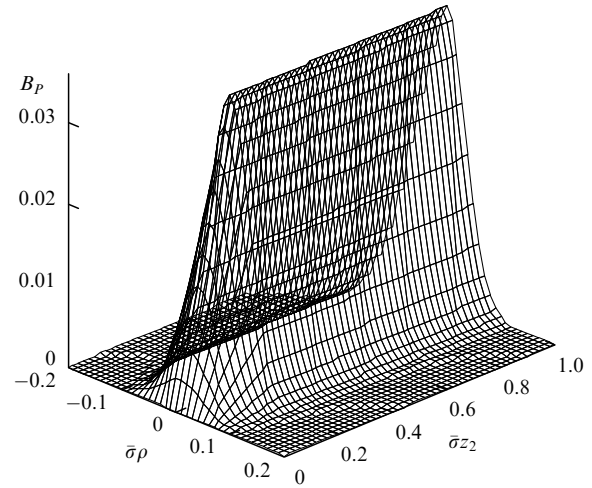


Figure 2. The function of spatial correlation B_P of relative fluctuations of tomographic signal power in a medium with a fluctuating absorption coefficient as a function of variables $\bar{\sigma}_\rho$ and $\bar{\sigma}_{z_2}$ for $\bar{\sigma}_{z_1} = 0.2$. The dispersion of fluctuations of absorption index is $d_\kappa = 0.5\bar{\sigma}^2$, and the correlation radius $\rho_\kappa = 0.05/\bar{\sigma}$.

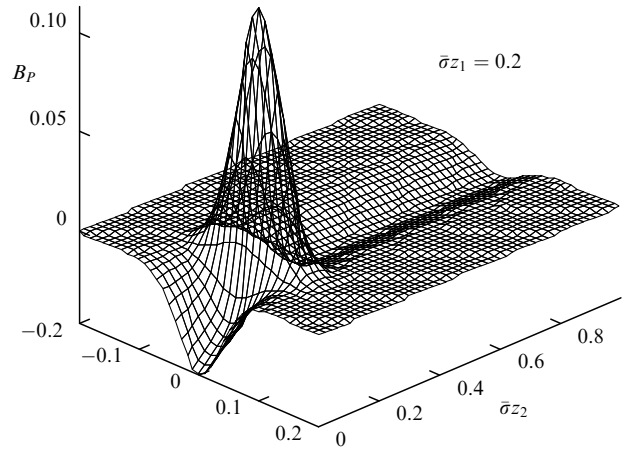


Figure 3. The same as in Fig. 2 but for a medium with a fluctuating backscattering coefficient for $d_\sigma = 0.125\bar{\sigma}^2$ and $\rho_\sigma = 0.05/\bar{\sigma}$.

were determined in addition to the dependence $d_P(z)$:

$$R(z_1, z_2) = \frac{B_P(0, z_1, z_2)}{\sqrt{d_P(z_1)}\sqrt{d_P(z_2)}},$$

$$\bar{B}_P(\rho, \xi) = \frac{1}{z_0} \int_0^{z_0} B_P \left(\rho, z + \frac{\xi}{2}, z - \frac{\xi}{2} \right) dz.$$

They correspond to the coefficient of longitudinal correlation of relative signal fluctuations and their correlation function averaged over the thickness z_0 of the medium layer under study. The data presented in Fig. 5 illustrate the possibility of fitting the theoretical predictions to experimental results by exhausting medium parameters appearing in formulas used and, in this way, the feasibility of determining them by the OCT method.

5. Conclusions

In this report we presented the problems of imaging theory, which effectively use the small-angle approximation of radiative transfer theory. The list could be further continued. However, it should be borne in mind that the accuracy of

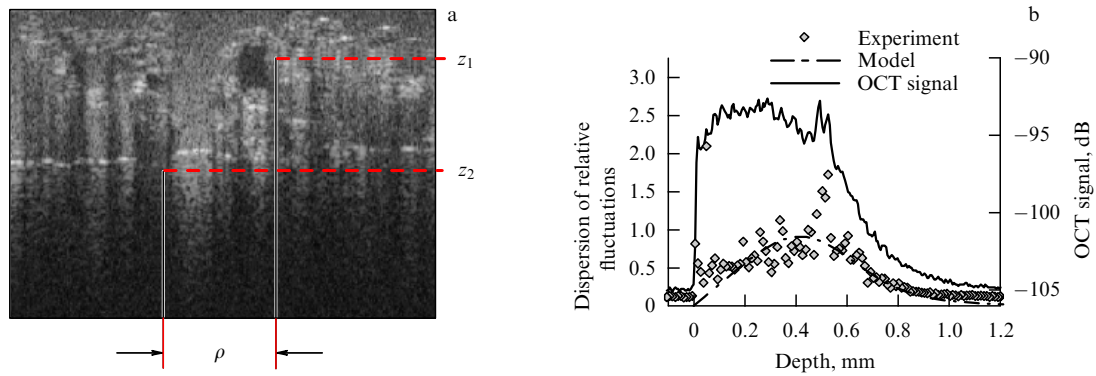


Figure 4. Tomogram of a model turbid medium (a) and results of its analysis (b). The solid line plots the mean power of the OCT signal as a function of depth, squares correspond to the dispersion of relative fluctuations of the measured signal, and the dashed curve presents the theoretical dependence of the dispersion of fluctuations on the depth.

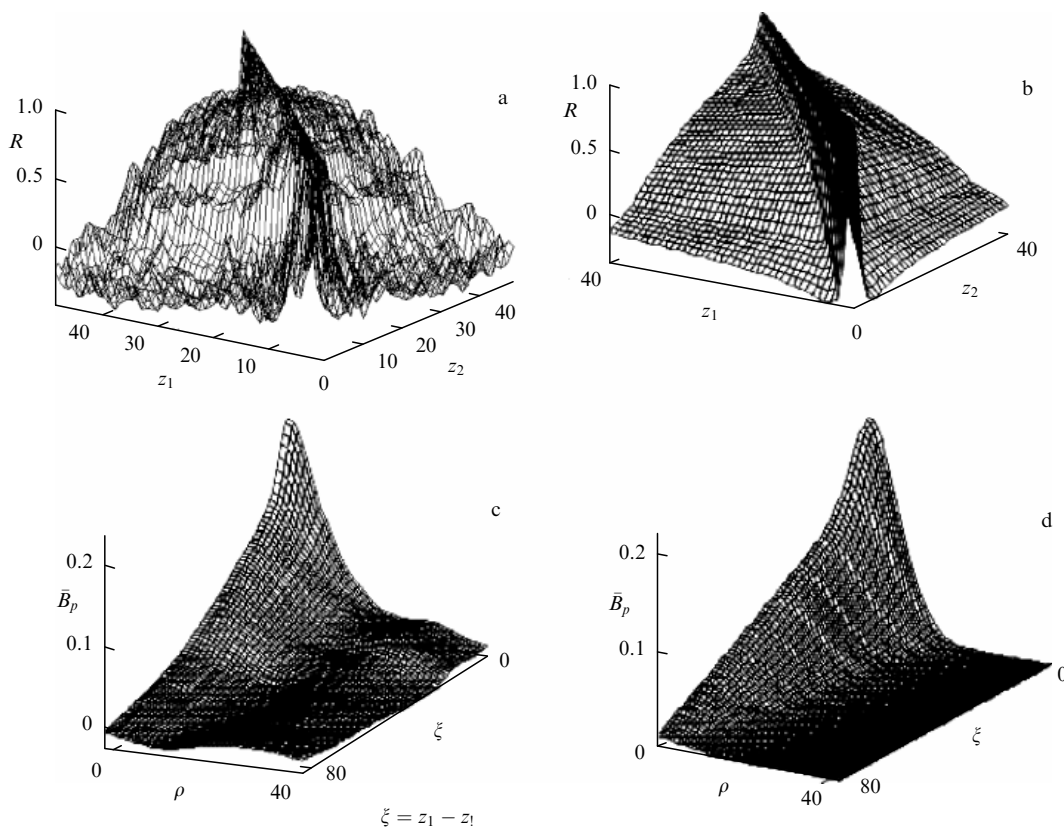


Figure 5. Correlation characteristics of the tomogram presented in Fig. 4: (a, b) the coefficient of longitudinal correlation $R(0, z_1, z_2)$ of image noise, and (c, d) the depth-averaged function of spatial noise correlation $\bar{B}_p(\rho, \xi)$. Panels (a) and (c) present the results of tomogram processing, and (b) and (d) display the theoretical results.

this approximation is strongly sensitive to the angular width of the scattering indicatrix and absorption ability of the medium. In seawater, for which the albedo of single scattering (A) is commonly below 0.9, this approximation performs reliably for optical thicknesses reaching up to $\tau \sim 15$. For biological tissues, where $A \sim 0.99$, the diffusive and directional components of irradiance in a narrow light beam become equal already at $\tau \sim 5$. This calls for hybrid models of the light field [12, 48], which allow for the effects of multiple light scattering over large angles.

The work was carried out with the support of the Russian Foundation for Basic Research (project No. 07-02-01179) and the grant 'Leading Scientific Schools of Russia' NSH-6043.2006.2.

References

1. Koshmider H *Beitrag Phys. Atm.* **12** (3) 171 (1925)
2. Duntley S Q *J. Opt. Soc. Am.* **53** 214 (1963)
3. Dolin L S *Izv. Vyssh. Uchebn. Zaved. Radiofiz.* **7** 380 (1964)
4. Bravo-Zhivotovskii D M, Dolin L S, Luchinin A G, Savel'ev V A *Izv. Akad. Nauk SSSR, Fiz. Atm. Okeana* **5** 160 (1969)
5. Levin I M *Izv. Akad. Nauk SSSR, Fiz. Atm. Okeana* **5** 62 (1969)
6. Bravo-Zhivotovskii D M, Dolin L S, Luchinin A G, Savel'ev V A *Izv. Akad. Nauk SSSR, Fiz. Atm. Okeana* **5** 672 (1969)
7. Bravo-Zhivotovskii D M et al. *Izv. Akad. Nauk SSSR, Fiz. Atm. Okeana* **7** 1143 (1971)
8. Ermakov B V, Il'inskii Yu A *Izv. Vyssh. Uchebn. Zaved. Radiofiz.* **12** 694 (1969) [*Radiophys. Quantum Electron.* **12** 554 (1969)]
9. Dolin L S, Savel'ev V A *Izv. Akad. Nauk SSSR, Fiz. Atm. Okeana* **7** 505 (1971)

10. Mertens L E, Replogle F S (Jr.) *J. Opt. Soc. Am.* **67** 1105 (1977)
11. Monin A S (Ed.) *Optika Okeana* (Oceanic Optics) (Moscow: Nauka, 1983)
12. Zege E P, Ivanov A P, Katsev I L *Perenos Izobrazheniya v Rasseyivayushchei Srede* (Image Transfer Through a Scattering Medium) (Minsk: Nauka i Tekhnika, 1985) [Translated into English (Berlin: Springer-Verlag, 1991)]
13. Dolin L S, Levin I M *Spravochnik po Teorii Podvodnogo Videniya* (The Theory of Underwater Vision. Handbook) (Leningrad: Gidrometeoizdat, 1991)
14. Dolin L S, Levin I M "Optics underwater", in *Encyclopedia of Applied Physics* Vol. 12 (Ed. G L Trigg) (New York: VCH Publ., 1995)
15. Dolin L S *Izv. Vyssh. Uchebn. Zaved. Radiofiz.* **7** 559 (1964)
16. Dolin L S, Thesis for Candidate of Sciences (Phys.-Math.) (Gor'ky: NIRFI, 1966)
17. Dolin L S *Izv. Vyssh. Uchebn. Zaved. Radiofiz.* **11** 840 (1968) [*Radiophys. Quantum Electron.* **11** 486 (1968)]
18. Rytov S M, Kravtsov Yu A, Tatarskii V I *Vvedenie v Statisticheskuyu Radiofiziku* Pt. 2 *Sluchainye Polya* (Principles of Statistical Radiophysics) (Moscow: Nauka, 1978) [Translated into English (Berlin: Springer-Verlag, 1989)]
19. Barabanenkov Yu N *Usp. Fiz. Nauk* **117** 49 (1975) [*Sov. Phys. Usp.* **18** 673 (1975)]
20. Apresyan L A, Kravtsov Yu A *Teoriya Perenosa Izlucheniya* (Radiation Transfer Theory) (Moscow: Nauka, 1983)
21. Sobolev V V *Perenos Luchistoi Energii v Atmosferakh Zvezd i Planet* (A Treatise on Radiative Transfer) (Moscow: Gostekhizdat, 1956) [Translated into English (Princeton, NJ: Van Nostrand, 1963)]
22. Huang D et al. *Science* **254** 1178 (1991)
23. Kravtsov Yu A, Saichev A I *Usp. Fiz. Nauk* **137** 501 (1982) [*Sov. Phys. Usp.* **25** 494 (1982)]
24. Dolin L S *Izv. Vyssh. Uchebn. Zaved. Radiofiz.* **41** 1258 (1998) [*Radiophys. Quantum Electron.* **41** 850 (1998)]
25. Vinogradov A G, Kravtsov Yu A *Izv. Vyssh. Uchebn. Zaved. Radiofiz.* **16** 1055 (1973) [*Radiophys. Quantum Electron.* **16** 811 (1973)]
26. Kompaneets A S *Zh. Eksp. Teor. Fiz.* **15** 235 (1945)
27. Molire V G *Z. Naturforsch. A* **3** 78 (1948)
28. Kompaneets A S *Zh. Eksp. Teor. Fiz.* **17** 1059 (1947)
29. Scott W T, Snyder H S *Phys. Rev.* **78** 223 (1950)
30. Dolin L S, Savel'ev V A *Izv. Vyssh. Uchebn. Zaved. Radiofiz.* **22** 1310 (1979) [*Radiophys. Quantum Electron.* **22** 911 (1979)]
31. Luchinin A G *Izv. Vyssh. Uchebn. Zaved. Radiofiz.* **14** 1925 (1971) [*Radiophys. Quantum Electron.* **14** 1507 (1971)]
32. Remizovich V S, Rogozkin D B, Ryazanov M I *Izv. Akad. Nauk SSSR, Fiz. Atm. Okeana* **19** 1053 (1983)
33. Dolin L S *Dokl. Akad. Nauk SSSR* **260** 1344 (1981) [*Sov. Phys. Dokl.* **26** 976 (1981)]
34. Furutsu K *J. Math. Phys.* **20** 617 (1979)
35. Dolin L S *Izv. Akad. Nauk SSSR, Fiz. Atm. Okeana* **16** 55 (1980) [*Izv. Acad. Sci. USSR, Atm. Oceanic Phys.* **16** 34 (1980)]
36. Dolin L S, Preprint No. 587 (Nizhny Novgorod: IPF RAN, 2001)
37. Luchinin A G *Izv. Akad. Nauk SSSR, Fiz. Atm. Okeana* **15** 770 (1979)
38. Veber V L *Izv. Vyssh. Uchebn. Zaved. Radiofiz.* **22** 989 (1979) [*Radiophys. Quantum Electron.* **22** 684 (1979)]
39. Mullamaa Yu-A R et al. *Stokhasticheskaya Struktura Polei Oblachnosti i Radiatsii* (Stochastic Structure of Cloudiness and Radiation Fields) (Tartu: Izd. AN ESSR, 1972)
40. Borovoi A G *Dokl. Akad. Nauk SSSR* **276** 1374 (1984) [*Sov. Phys. Dokl.* **29** 490 (1984)]
41. Dolin L S *Dokl. Akad. Nauk SSSR* **277** 77 (1984) [*Sov. Phys. Dokl.* **29** 544 (1984)]
42. Fukshansky L J. *Quant. Spectrosc. Radiat. Transfer* **38** 389 (1987)
43. Kliorin N I et al. *Izv. Vyssh. Uchebn. Zaved. Radiofiz.* **32** 1072 (1989) [*Radiophys. Quantum Electron.* **32** 793 (1989)]
44. Dolin L S *Izv. Vyssh. Uchebn. Zaved. Radiofiz.* **49** 799 (2006) [*Radiophys. Quantum Electron.* **49** 719 (2006)]
45. Dolin L S, Shchegol'kov Yu B, Shchegol'kov D Yu *Izv. Vyssh. Uchebn. Zaved. Radiofiz.* **51** 247 (2008) [*Radiophys. Quantum Electron.* **51** 222 (2008)]
46. Dolin L S, Sergeeva E A, Turchin I V *Kvantovaya Elektron.* **38** 543 (2008) [*Quantum Electron.* **38** 543 (2008)]
47. Dolin L S, Turchin I V, Preprint No. 750 (Nizhny Novgorod: IPF RAN, 2007)
48. Gelikonov G V, Dolin L S, Sergeeva E A, Turchin I V *Izv. Vyssh. Uchebn. Zaved. Radiofiz.* **46** 628 (2003) [*Radiophys. Quantum Electron.* **46** 565 (2003)]